Studies on Age-related Changes of Lipid Metabolisms

January 2021

Ayumi ANDO

Studies on Age-related Changes of Lipid Metabolisms

A Dissertation Submitted to
the Graduate School of Science and Technology,
University of Tsukuba
in Partial Fulfillment of Requirements
for the Degree of Doctor of Philosophy in Science
Doctoral Program in Biology,
Degree Programs in Life and Earth Sciences

Ayumi ANDO

Table of contents

Abstract **3**

Abbreviations **5**

General Introduction **7**

Chapter 1: Deoxysphingolipids and ether-linked diacylglycerols accumulate in the tissues of aged mice **10**

Abstract 11

Introduction 12

Material and Methods 14

Results and discussion 20

Tables and Figures 27

Chapter 2: A Simple and Highly Sensitive Quantitation of Eicosanoids in Biological Samples Using Nano-flow Liquid Chromatography/Mass Spectrometry **34**

Abstract 35

Introduction 36

Material and methods 39

Results and Discussion 43

Tables and Figures 48

Acknowledgements **55**

References **56**

Abstract

Senescence is known as a risk factor in multiple diseases such as neurodegenerative disorders and diabetes, and its physiological increase is known as aging. Therefore, studies exploring the underlying mechanisms of senescence are expected to lead to the discovery of new drug targets and biomarkers in these diseases. However, because of the multiple mechanisms contributed to the aging process, narrow down the cause of aging. Therefore, molecular network analysis have been used to understanding this process. One such type is metabolomic analysis, which provides qualitative and quantitative information regarding all metabolites in a cell, tissue, or organ. Therefore, metabolomic studies have the potential to provide valuable insights into the mechanisms of senescence and senescence-related diseases. Various reports carried out metabolic approaches to evaluate the aging organs of aged mammals, however the cause of physiological decline, i.e., senescence, with aging is still unclear.

In the first chapter, I described comprehensive analysis for hydrophilic and hydrophobic metabolites by LC/MS and GC/MS to evaluate changes in metabolism associated with aging, especially lipid metabolism about each from various organs. As a result, more than 1,000 metabolites were statistical analysis was carried out and deoxysphingolipids and ether-bound diacylglycerols were found in aged mouse tissues as age-related lipids. Deoxysphingolipids were reported to increases in the serum with the associate of neurological symptom of drug-induced adverse effect. And also increases has been reported in the plasma of metabolic syndrome and related disorders. As for the ether-linked, I speculated the cause of increases of ether-linked diacylglycerol was degradation of ethanolamine plasmalogen, which has ether-bound glycerol structure. These finding indicated that the aging-associated lipids, and their possible role in senescence could be

investigated. this study will contribute to the understanding of the aging process and the prevention of accelerated aging and aging-associated diseases.

In chapter 2, I had carried out the development of an analytical method of simple and highly sensitive quantitation of eicosanoids using nano-flow liquid chromatography/mass spectrometry. Generally, simultaneous lipid analysis could not detect the picomolar level lipids. However, inflammation disease such as arteriosclerosis is deeply modulated by the picomolar and femtomolar levels of bioactive lipids called eicosanoids. However, the sample preparation processes for these lipids are laborious and time-consuming tasks, and the data quality relies largely on skill and experience. To solve these problems, I established a simple sample preparation using a phospholipid-removal solid-phase extraction column. As a results, the quantitation range achieved 0.01 – 100 ng/mL for thromboxane B_2, and 0.05 – 100 ng/mL for prostaglandin E_2, prostaglandin D_2, prostaglandin F_2, leukotriene B_4, 6-keto prostaglandin $F_{1\alpha}$ and 11-dehydro thromboxane B_2. The minimized sample preparation contributes for the analytical robustness.

Taken together, I conclude that the changes of age-related unique lipids were possible to associate with aging related disorder, and the simple and high sensitivity with robustness was achieved which will be enable to evaluate more precise metabolism changes.

Abbreviations

Deoxydihydroceramide	doxDHCer
Deoxyceramide	doxCer
Diacylglycerol	DAG
Coenzyme A	CoA
Serine palmitoyltransferase	SPT
Plasmalogen-selective phospholipase A2	PSPLA2
L-serine	L-Ser
L-alanine	L-Ala
Platelet-activating factors	PAFs
Gas chromatography-mass spectrometry	GC/MS
Enzyme-linked immunosorbent assays	ELISA
Nano-flow Liquid Chromatography	Nano-LC
Mass Spectrometry	MS
Electrospray ionization	ESI
Ultra-fast liquid chromatography	UFLC
Ultra performance liquid chromatography	UPLC
Liquid Chromatography with tandem mass spectrometry	LC-MS-MS
Solid-phase extraction	SPE
Liquid-liquid extraction	LLE
Prostaglandin E_2	PGE_2
Prostaglandin D_2	PGD_2
6-keto prostaglandin $F_{1\alpha}$	6-keto $PGF_{1\alpha}$
Prostaglandin $F_{2\alpha}$	$PGF_{2\alpha}$

Leukotriene B_4	LTB_4
Thromboxane B_2	TXB_2
11-dehydro thromboxane B_2	11-dehydro TXB_2
Selected reaction monitoring mode	SRM
Full-width at the half-maximum	FWHF

General Introduction

Aging is defined as a decline in cellular function. Therefore, all living organisms can`t live forever, even if the lifespan is long or short. It is an inevitable process that eventually occurs in all living organisms. However, if there is a group of the same chronological age, I can see a variety of biological aging in there. Accelerated aging causes disorders such as atherosclerosis, cataracts, diabetes, osteoporosis, cancer, and muscle wasting.

Interestingly, research on the detection of accelerated aging in young adults using 18 biomarkers has enabled us to note the differences in individuals with aging speed. A lot of researchers had been reporting to evaluate this unavoidable phenomenon. However, it was unable to concentrate on a single target because there are some biological backgrounds; 1. living things have complicated metabolism processes in their body. 2. endogenous metabolites are influenced by environmental factors (e.g., smoking, exercise, dietary habits) is different in individuals. 3. Genetic variation included in single nucleotide polymerase is underlying and affect metabolism. According to these backgrounds, there are 4 types of suggestion of cause of senescence until now; 1. Lifetime program theory: Abnormal telomere maintenance mechanism, 2. Accumulation of DNA damage: Mutations in the mitochondrial genome and consequent mitochondrial respiration abnormalities, *etc*. 3. Metabolic disorders due to accumulation of *in vivo* molecules such as abnormal proteins: Oxidation, sugar chain modified protein, *etc*. 4. Tissue damage, such as collapse of tissue flexibility due to abnormal cross-linking of collagen and elastin.

For these wide varieties of reasons, understanding of senescence mechanism is not simple, hence a comprehensive understanding of the molecular mechanism of

senescence is a huge theme of bioscience. To approach this theme, a comprehensive analysis using mass spectrometry has been applied as one of the tools to understand multiple molecular networks in recent years. For example, a combination of gene expression and metabolomic analyses has provided a footprint of aging in mice. These analyses demonstrated decreased long-chain acylcarnitine levels, increased free fatty acid levels, and marked reduction in various amino acid levels in the plasma of aged mice. Furthermore, in addition to the less identified lipid- and disease-specific or single organ analysis, the lipidomics approach has been reported for aging and aging-related diseases.

Lipids provide important play important roles in inflammation, Signal transduction, maintain mitochondria, and ion channel control. For example, Sphingolipids and diacylglycerol are a class of lipids that are intricately involved in numerous cell processes, including proliferation, senescence, differentiation, and signaling.

Degradation of phospholipids by phospholipase generate fatty acid, such as polyunsaturated fatty acid. The metabolites of arachidonic acid generate eicosanoids which control inflammation, the aging process encompasses changes at the molecular, caller and pathological changes that have been analyzed by various methods. In the recent decade, omics approaches to understanding aging biology try to explain how changes the aging metabolism compared to the young it and how changes in function can affect by mass spectrometry.

However, the cause of physiological decline with aging is still unclear. Furthermore, in addition to the less identified lipid- and disease-specific or single organ analysis, the lipidomics approach has been reported for aging and aging-related diseases.

Therefore, in chapter 1, I described about the changes in metabolism with aging, particularly the changes in lipid metabolism, I analyzed the metabolomes and lipidomes of the cerebral cortex, liver, femoral muscle, and epididymal fat in young mice. As a result, more than 1,000 molecules were detected, and I identified deoxyceramide (doxCer), deoxysphingolipid (doxDHCer), and ether-linked diacylglycerols as aging-associated lipids. The doxDHCer and doxDHCer are reported as deoxy-sphingolipids family, which increase in the serum from type2 diabetes patients and metabolic syndrome patients. As for the ether-linked diacylglycerol, the lack of ether lipids has been reported to reduce the amount and release of neurotransmitters in the mice. Taken together, these lipids might associate with senescence-related symptoms. However, this is the first report on aging from the point of view of lipid study. From this result, more deep studies are required to evaluate these phenomena.

In chapter 2, I conducted out the development of an analytical method of simple and highly sensitive quantitation of eicosanoids using nano-flow liquid chromatography/mass spectrometry. Generally, simultaneous lipid analysis could not detect the picomolar level lipids. However, inflammation disease such as arteriosclerosis is deeply modulated by the picomolar and femtomolar levels of bioactive lipids called eicosanoids. However, the sample preparation processes for these lipids are laborious and time-consuming tasks, and the data quality relies largely on skill and experience. To solve these problems, I established a simple sample preparation using a phospholipid-removal solid-phase extraction column. This method showed acceptable robustness and sensitivity. This approach can be expanded to other metabolites that require highly sensitive analysis.

Chapter 1: Deoxysphingolipids and ether-linked diacylglycerols accumulate in the tissues of aged mice

Abstract

Senescence is a well-known risk factor for several diseases, such as neurodegenerative disorders. Therefore, studies exploring the mechanisms underlying aging are expected to guide the discovery of novel drug targets and biomarkers for these diseases. However, a comprehensive overview of the metabolic and lipidomic changes in healthy aging mammals is lacking. To understand the changes of metabolism with aging, especially lipid metabolism, I analyzed the metabolomes and lipidomes of the cerebral cortex, liver, femoral muscle, and epididymal fat in young and aged mice. Two-dimensional cluster analysis revealed clear separation between the metabolite profiles of the aged and young groups. Deoxydihydroceramide (doxDHCer), deoxyceramide (doxCer), and ether-linked diacylglycerol (DAG) levels were elevated during aging. This is the first report of age-related variations in deoxysphingolipid and ether-linked DAG levels in mice. DoxCer, doxDHCer, and ether-linked DAGs may be associated with senescence in mammalian tissues.

Introduction

Senescence underlies a wide range of diseases, such as cancer and neurodegenerative, cardiovascular, and metabolic diseases (López-Otín *et al*., 2013). Studies clarifying the mechanisms of senescence are expected to guide the discovery of novel drug targets and biomarkers for these diseases. Understanding the molecular mechanisms of senescence could facilitate the identification of biomarkers of biological age. Furthermore, given the underlying multisystem network underlying the aging process, with changes occurring at molecular and organ-based levels, biological plausibility suggests that no single biomarker is likely to completely explain biological age.

Because multiple mechanisms contribute to the occurrence of senescence, molecular network analysis has been frequently used to comprehensively understand this process (López-Otín *et al*., 2013; Petrosillo *et al*., 2008; Houtkooper *et al*., 2011). One such type is metabolomic analysis, which provides qualitative and quantitative information regarding all metabolites in a cell, tissue, or organ. Therefore, metabolomic studies have the potential to provide valuable insights into the mechanisms of senescence and senescence-related diseases. For instance, recent studies summarizing a combination of gene expression and metabolomic analyses have provided a footprint of aging in mice (Houtkooper *et al*., 2011; Seo *et al.*, 2016). These analyses demonstrated decreased long-chain acylcarnitine levels, increased free fatty acid levels, and marked reduction in various amino acid levels in the plasma of aged mice.

Additionally, research on the detection of accelerated aging in young adults using 18 biomarkers have enabled to note the differences in individuals with aging speed. This study has mentioned metabolic changes and physiological decline with aging by

analyzing biomarkers (Belsky *et al*., 2015). However, the cause of physiological decline, i.e., senescence, with aging is still unclear. Furthermore, in addition to the less identified lipid- and disease-specific or single organ analysis, the lipidomics approach has been reported for aging and aging-related diseases (Tu *et al*., 2017; Braun *et al*., 2016).

In this study, to clarify the changes in metabolism with aging, particularly the changes in lipid metabolism, I analyzed the metabolomes and lipidomes of the cerebral cortex, liver, femoral muscle, and epididymal fat in young (9 weeks old) and aged (114 weeks old) mice. A comprehensive analysis revealed previously unidentified metabolic changes that represented age-related variations in deoxydihydroceramide (doxDHCer), deoxyceramide (doxCer), and ether-linked diacylglycerol (DAG) levels in aged mice. These novel findings in the fields of molecular biology and senescence may provide further insight into aging-related diseases.

Material and Methods

Reagents

Acetonitrile, isopropanol, methanol, acetic acid, formic acid (all LC/MS grade), octylamine, 2 M ammonia isopropanol solution, 0.2 M disodium dihydrogen ethylenediaminetetraacetic acid (EDTA-2Na) solution, and pyridine were purchased from Wako Pure Chemicals (Osaka, Japan). The amino acid standard solution was purchased from Agilent Technologies Inc. (Santa Clara, CA, USA). Methoxyamine hydrochloride, N,O-bis(trimethylsilyl)trifluoroacetamide (BSTFA) and trimethylchlorosilane (TMCS) (99:1) mixed in solvent; algal amino acid mixture (U-^{13}C); and N-tert-butyldimethylsilyl-N-methyltrifluoroacetamide with 1% tert-butyldimethylchlorosilane (MTBSTFA with 1% t-BDMCS) were purchased from Sigma-Aldrich (St. Louis, MO, USA).

Animals

Six-week-old C57BL/6J mice were purchased from CLEA (Tokyo, Japan) and housed in groups of four in a temperature-controlled facility with a 12-hour light/12-hour dark schedule. Mice in the aged group received standard chow (CE-2, CLEA) and water ad libitum until 111 weeks of age. Under the same conditions, young mice were acclimatized for 7 days, until they reached 7 weeks of age. All mice were weighed before the day of investigation and before the start of the experiment. Food intake can affect metabolomic data; therefore, after overnight fasting (16 hours), all the mice were reweighed and sacrificed by decapitation for sample collection. Tissue collection were carried out within 3 min and collected tissues were into 2.0mL test tube and immediately frozen by liquid nitrogen then weighed. For plasma preparation, for biochemical analysis, EDTA-2Na (150 mM, pH 7.4) were added 5% (v/v) to collected blood, followed by

immediate centrifugation (10,000× g 10 min, 4 °C). All samples were stored -80 °C until use. All animal experiments were conducted in accordance with a protocol reviewed and approved by the Institutional Animal Care and Use of Takeda Pharmaceutical Co., Ltd.

Biochemistry

Glutamic pyruvic transaminase (GPT) activity and glucose (Glu), total ketone body (T-KB), total cholesterol (T-CHO), and triglyceride (TG) levels were determined in plasma using a Hitachi 7180 autoanalyzer (Hitachi High-Technologies Corp., Tokyo, Japan).

Global metabolomic analysis

Sample preparation

Global metabolomic profiles were obtained by combining data derived from the following platforms: liquid chromatography-tandem mass spectrometry (for lipidomics; LC/MS), gas chromatography with mass spectrometry (GC/MS), amino acid quantification, and ion-pair liquid chromatography-tandem mass spectrometry (IP-LC/MS/MS).

Tissues were homogenized in isopropanol (100 mg/mL) for lipidomics and in methanol (100 mg/mL) for GC/MS, amino acid quantification and IP-LC/MS/MS using a ShakeMaster Auto instrument (BioMedical Science, Tokyo, Japan). Homogenization was followed by centrifugation at 15,000 rpm for 5 min. During these processes, the samples were kept in an ice-cold tube. The mixed quality control (mixQC) samples were prepared by mixing aliquots of the each tissue homogenates, then followed by centrifugation by as same as above condition. Precision, referred to the coefficient of

variation, was calculated using five times repeated analysis data of mixQC. Metabolite and lipid showing a coefficient of variation less 30% was adopted.

Lipidomics

Five microliters of each sample (supernatants from the isopropanol homogenate) was injected onto a XBridge C18 column (2.1×50 mm, 3 μm; Waters Corp., Milford, CT, USA). Chromatographic separation was performed on an Ultimate3000 RSLC LC/MS system (Thermo Fisher Scientific Inc., Sunnyvale, CA, USA) using a gradient elution consisting of mobile phase A (0.01% acetic acid and 1 mM ammonia in MilliQ water) and mobile phase B (0.001% acetic acid and 0.2 mM ammonia in ethanol/isopropanol [3:1]) at a flow rate of 0.7 mL/min. The following gradient program was used: 0-2 min, 2% B; 2-10 min, 2-100% B; 10-12 min, 100% B; and 12-15 min, 2% B. Analysis was performed using an Orbitrap XL mass spectrometer (Thermo Fisher Scientific Inc.) operated at 60,000 full width at half maximum in both positive and negative ionization modes. Raw LC/MS data were processed using Expressionist Refiner MS software, version 8.2 (Genedata AG, Basel, Switzerland). Lipids were identified based on their molecular mass and retention time on an HPLC chromatograph (Satomi, Hirayama, and Kobayashi 2017). The data including monoisotopic m/z value and retention time information were exported, and further processing was performed using Excel.

IP-LC/MS/MS

The LC/MS/MS system consisted of a Nexera HPLC system (Shimadzu Co., Kyoto, Japan) and a 5500 QTRAP mass spectrometer (AB Sciex Pte., Ltd., Toronto, Canada). Ten microliters of each sample (supernatants from the methanol homogenate)

was injected onto an Atlantis T3 reversed-phase column (2.1×100 mm, 3 μm, 130 Å; Waters Corp.) maintained at 35°C, and chromatographic separation was performed using a gradient elution (0-2 min, 1% B; 2-12.5 min, 1-100% B; 12.5-15 min, 100% B; 15-27 min, 1% B) consisting of mobile phase A (0.1% octylamine, 0.07% acetic acid and 10 μM EDTA-2Na in MilliQ water) and mobile phase B (0.07% acetic acid in methanol/isopropanol [4:1]). All target molecules were observed in the multiple reaction monitoring (MRM) mode with simultaneous polarity switching. The MRM conditions were as previously described (Yuan *et al.*, 2012). The LC/MS/MS data were processed by MultiQuant software (AB Sciex Pte., Ltd., Toronto, Canada).

GC/MS

Fifty microliters of each sample (supernatants from the methanol homogenate) was dried under a nitrogen stream. The dehydrated supernatant was then subjected to a derivatization reaction by adding 50 μL of methoxyamine hydroxychloride in pyridine (15 mg/mL) and incubating at 30°C for 30 min. This step was followed by a second derivatization reaction, in which 100 μL of trimethylsilylation reagent was directly added to the first reaction mixture and incubated at 60°C for 30 min. The reaction mixture (1 μL) was injected into an Agilent 7890A GC system for chromatography in splitless injection mode using a GC Injector 80 autosampler (Agilent Technologies Inc., Santa Clara, CA, USA). GC separation was performed on a J&W Scientific HP-5MS-DG column (30 m × 0.25 mm × 0.25 μm; Agilent Technologies) using a temperature gradient, with the temperature increasing from 60°C to 325°C at 10°C/min, with a consistent helium gas flow of 1 mL/min. The eluate was ionized via electron impact ionization (70 eV) with an ion-source temperature of 280°C and introduced into an Agilent 5975C mass

spectrometer. Each target molecule was detected in full-scan mode, and metabolite annotation was performed by Fiehn Metabolomics Library (Agilent Technologies).

Amino acid quantification

For amino acid quantification, tert-butyldimethylsilyl (tBDMS) derivatization for GC/MS analysis was performed. For sample preparation, supernatants (50 μL) from the methanol homogenates were mixed with 10 μL of internal standard (IS) solution in a glass vial and dried under a nitrogen stream. Next, the dehydrated supernatant was subjected to a derivatization reaction by adding 50 μL of a 1:1 solution of MTBSTFA (with 1% t-BDMCS) and acetonitrile. The glass vial was tightly capped and incubated at 70°C for 180 min. Finally, 10 μL of derivatized solution was used for GC/MS analysis. Calibration standards were prepared by diluting the standard stock solution in methanol at final concentrations of 0.1, 1, 10, 25, 50, 100, and 125 nmol/mL for all the amino acids and 0.4 mg/mL for the IS. Methanol (50 μL) was added to a glass tube with 10 μL of IS solution, and derivatization was performed as described above. The calibration curve was prepared by the least-square linear regression method with 1/x weighting.

Statistical analysis

The fold changes in metabolite levels between the aged and young groups were calculated as ratios of the peak area values of each metabolite. Raw mass spectrometric data from IP-LC/MS/MS and lipidomics were performed using "R" (http://cran.r-project.org/) for two-dimensional cluster analysis and heat-map visualization after z score-standardized (mean 0 [SD 1]). The data shown in the figures are presented as volcano plots, with fold changes indicated using peak areas and p-values and outliers

represented as small symbols. Welch's t-tests were performed for statistical comparisons between young and old mice; $p < 0.05$ was considered significant.

Results and discussion

Aged mice exhibited elevated levels of doxDHCer in epididymal fat

The total body weights and biochemical parameters of the young and aged mice were assessed in parallel to confirm the phenotyping data. Body weights, glucose, and total ketone body levels (Table 1) were consistent with the results of a previous report comparing aged (22 months old) and young (3 months old) mice (Houtkooper *et al*., 2011). I used metabolomic and lipidomic techniques to analyze the cerebral cortex, liver, femoral muscle, and epididymal fat tissues in aged and young C57BL/6J mice [see Material and method] to understand the molecular mechanisms of senescence, and I identified more than 1000 metabolites in these tissues. The reasons for selecting these organs are as follows: 1) Femoral muscle and liver: these organs are the most energy-generating/consuming organs; therefore, I hypothesized that energy consumption affects aging; 2) Cerebral cortex: cognitive dysfunction is also known to be associated with aging, so I selected the cerebral cortex; and 3) Epididymal fat: Increase in body weight (especially fat) is associated with aging.

However, no researcher has investigated the changes in body fat in association with these conditions. I hypothesized that increase in body fat is associated with the accumulation or generation of abnormal molecules in the fat tissue. Cardiolipins, ceramides, cholesterol esters, glycerolipids, dolichols, carnitines, ubiquinones, fatty acyl coenzyme A (CoA), free fatty acids, and ganglioside were identified by lipidomic analysis and metabolites from the tricarboxylic acid cycle, glycolysis, sugars, bile acids, pyrimidine pathway, nicotinate, and nicotinamide pathway amino acids and their metabolites were identified by metabolomic analysis [see Additional file 3. (https://cellandbioscience.biomedcentral.com/articles/10.1186/s13578-019-0324-9)].

Then, the profiles of aged and young mice were compared, and cluster analysis revealed clear differences in terms of these profiles between these two groups. However, it was difficult to visualize the results because numerous metabolites were present in the results of cluster analysis. Therefore, I performed re-analysis to focus on deoxysphingolipids (doxSLs) and ether-linked DAGs. I could not find any report regarding the relationship between aging and these lipids at the time of data analyses. Thus, I chose doxSLs and ether-linked DAGs as focused metabolites. They were chosen as unique metabolites in aging for subsequent analyses.

From cluster analysis, I also identified unique molecular species of ether-linked DAGs and sphingolipids in aged mice that varied from the ceramide species generally found in the epididymal fat tissues, cerebral cortex, and liver. I observed higher ether-linked DAG levels in the cerebral cortex, fat tissue, and liver of the aged mice than in equivalent tissues of young mice (Figs. 1a–c). The femoral muscle showed no significant changes (Fig 2). Furthermore, the doxCer levels were significantly higher ($p < 0.05$, fold change > 1) in the epididymal fat tissues (Fig. 3a) and cerebral cortex of aged mice than in the equivalent tissues in young ones. Moreover, doxDHCer levels were significantly higher in the epididymal fat tissues (Fig. 3b). These doxSLs have been identified in the plasma of patients with hereditary sensory and autonomic neuropathy (Penno *et al*., 2010). The levels of two types of doxSL, i.e., doxCer and doxDHCer, were significantly higher in the epididymal fat tissue of aged mice than those in young ones (Fig 4 and 5). Conversely, in the cerebral cortex, doxCer levels were higher but doxDHCer levels were lower in aged mice than those in young ones. Further, significant differences were not observed in the levels of these molecules in the liver or femoral muscle.

These molecules are synthesized by serine palmitoyltransferase (SPT), with the preferred substrates being serine and palmitoyl-CoA. SPT catalyzes the condensation of L-serine (L-Ser) and palmitoyl-CoA to form 3-keto-sphinganine and ultimately sphinganine. Sphinganine is subsequently N-conjugated with a second fatty acid to form dihydroceramide. Moreover, SPT can use L-alanine (L-Ala), as a substitute, and conjugated alanine forms doxSLs (Esaki *et al*., 2015) via 1-deoxysphinganine and 1-deoxysphingosine. In an *in vitro* study, doxSLs, such as doxCer and doxDHCer, were generated in the presence of high L-Ala/L-Ser ratios in the lipid droplets in cells (Esaki *et al*., 2015). Based on this information, I analyzed L-Ser and L-Ala levels in several tissues to clarify the reason for their accumulation in epididymal fat.

Epididymal fat tissues displayed no changes in L -Ser and L-Ala levels

I analyzed L-Ser and L-Ala levels in the liver, cerebral cortex, epididymal fat, and femoral muscle tissue in aged and young mice to determine whether the L-Ala/L-Ser ratio changed with aging via amino acid quantification (Fig. 3c). The aged mice exhibited lower L-Ser levels in the liver and cerebral cortex as well as lower L-Ala in the cerebral cortex and femoral muscle than those in young ones. Conversely, no changes were observed in the epididymal fat.

Nevertheless, lower L-Ser and L-Ala levels and higher doxCer and dosDHCer levels in the epididymal fat than those in the other tissues were observed. There were no changes between aged and young mice with respect to the L-Ala/L-Ser ratio, which was 0.9–1.13. In addition, the standard deviation of the L-Ala/L-Ser ratio was lower than the individual values of L-Ala and L-Ser in all tissues. I hypothesize that these phenomena are attributable to the accumulation of doxCers and doxDHCers in epididymal fat rather

than *de novo* synthesis because I did not observe differences in L-Ser levels and observed lower L-Ser levels in epididymal fat than in the other tissues.

In the cerebral cortex, significantly lower L-Ser and L-Ala levels were observed in aged mice than in young ones (Fig. 3c). A previous report found that the L-Ala/L-Ser ratio is a likely determinant of doxSL production; however, L-Ser levels were significant reduced in the cerebral cortex. Regarding the decreases in doxDHCer levels in the cerebral cortex, I speculate that there are two reasons for this: First, the lower L-Ala and L-Ser levels in the aged group than in the young group may have reduced the total production of doxDHCer. Second, the suppression of the enzyme activity, including serine palmitoyltransferase, 3-dehydrosphinganine reductase, and ceramide synthetase in the ceramide *de novo* synthesis until doxDHCer in the aged group, may also affect the total production of doxDHCer. Regarding the increase in doxCer levels in the cerebral cortex of the aged group, I speculate that the activation of the sphingolipid salvage pathway is one possible cause of the increase in doxCer levels.

Because the decreases in doxDHCer levels had already been observed, I speculate that doxCer synthesis from the *de novo* synthesis pathway is less likely. The use of enzyme activity to evaluate the decrease in doxDHCer levels in the brains of aged mice may be a useful method in understanding this phenomenon.

Recently, some reports have described an association between doxSLs and diseases; for example, patients with aberrant plasma L-Ser and L-Ala levels, a situation which can be secondary to mitochondrial disorders, exhibit peripheral neuropathy with similar elevated levels of atypical sphingolipids (Ferreira *et al.*, 2018). Further, doxSL levels are elevated in type 2 diabetes mellitus (Bertea *et al*., 2010), and such compounds are cytotoxic for insulin-producing cells (Zuellig *et al.*, 2014). These symptoms are similar to those of

aging-associated diseases that are caused by the progressive loss or dysfunction of cells. Based on the findings of our study and those from the abovementioned reports, I believe that further studies are warranted to understand age-related diseases and doxSLs. These studies indicate that the intracellular metabolites of deoxysphinganine, particularly doxDHCer, are important cytotoxic mediators (Zuellig *et al*., 2014; Kramer *et al*., 2015). To our knowledge, the present study is the first reporting age-related variations in doxCer and doxDHCer levels *in vivo*.

Increase in ether-linked DAG levels in aged tissues

I found that ether-linked DAG levels were significantly higher ($p < 0.05$, fold change > 1) in the epididymal fat tissues, cerebral cortex, and liver of aged mice than the equivalent tissues in young ones (Fig. 6). However, the detailed biosynthetic pathway for ether-linked DAGs has not been determined in aged mammals.

The first step in the synthesis of ether–lipids occurs in peroxisomes. Most phospholipids contain a hydrophobic fatty acid and hydrophilic phosphoglycerol head group. Conversely, ether-linked phospholipids contain long-chain fatty alcohols connected by an ether bond to the phosphoglycerol structure (Shevchenko and Simons 2010). Plasmalogen and platelet-activating factor (PAF) are the members of the latter group of lipid structures, with ethanolamine or choline being bonded as a head group to a fatty acid ether that is bonded to a fatty acid ester, which is in turn bonded to a glycerol skeleton (Nagan and Zoeller, 2001). Furthermore, PAF concentration is lower than that of ethanolamine plasmalogens (Shevchenko and Simons, 2010; Nagan and Zoeller, 2001; Latchoumycandane *et al*., 2015). Therefore, I hypothesized that the observed decrease in ethanolamine plasmalogen levels is caused by the elimination of this head group.

Analysis of the fold change in ethanolamine plasmalogen levels in aged and young mice (Fig. 3) revealed a significant decrease in its levels in aged mice, particularly in the cerebral cortex and epididymal fat tissues, and this decrease was accompanied by an increase in ether-linked DAG levels. Ether-linked diglyceride species, in contrast to ester-linked diglyceride species, do not activate protein kinase C (Musial *et al*., 1995) and ether-linked DAGs can induce growth arrest, but not apoptosis, in vascular/aortic cell lines (Houck *et al*., 2008).

The mechanisms underlying the accumulation and biosynthesis of ether-linked DAGs in aged mammals are unknown. The lipid profile observed in our analysis predicts that ethanolamine plasmalogens are the substrates of ether-linked DAGs.

Plasmalogen levels in the brain are reduced in patients with Alzheimer's disease (Ginsberg *et al*., 1995) and those with neurological injuries, including ischemia and spinal cord trauma (Farooqui and Horrocks, 2001). A previous report suggested that the stimulation of plasmalogen-selective phospholipase A2 (PSPLA2) caused this phenomenon, and plasmalogen degradation by PSPLA2 resulted in the generation of arachidonic acid, eicosanoids, and PAFs (Farooqui and Horrocks, 2001). In the present study, plasmalogen levels reduced in the cerebral cortex, whereas ether-linked DAG levels increased. Moreover, ether–lipid levels are reportedly elevated in human tumors, making such tumors more aggressive (Benjamin *et al*., 2013). A recent study has evaluated the alkylglycerone phosphate synthetase enzyme activities promotes tumor growth, which in the peroxisomally localized activities promotes tumor growth (Benjamin *et al*., 2013). Furthermore, the investigation of the relationship of growth arrest and apoptosis with ether-linked DAG levels may provide insights into healthy aging.

I hypothesize that ethanolamine plasmalogen hydrolysis increases ether-linked DAG levels in the cerebral cortex and epididymal fat tissues. Ether-linked DAGs have been identified in mammalian tissues such as the mouse brain and heart (Yang *et al.*, 2015); however, quantitative changes in its levels in aged animal models have not yet been reported. Therefore, further studies on the biological functions of ether-linked DAGs are warranted to determine whether these molecules play a role in the aging process.

I identified doxDHCer, doxCer, and ether-linked DAGs as aging-associated lipids, and their possible role in senescence could be investigated. Although some metabolic changes associated with aging have previously been investigated, to the best of our knowledge, this is the first time that changes in the levels of these three lipids have been unambiguously demonstrated using mass spectrometry. However, further research is needed to fully establish the relevance of these lipids to aging and clarify the biosynthesis of the newly identified age-related lipids. In addition, two questions need to be answered in future studies. First, what is the significance of the decrease in doxDHCer levels in the cerebral cortex? Second, can doxDHCer, doxCer, and ether-linked DAG levels be detected in the plasma of aged mammals? In this study, I could not conduct lipidomic analysis of plasma because of low sample amounts. If the plasma levels of doxDHCer, doxCer, and ether-linked DAGs can be detected, these data may provide insights into healthy senescence and facilitate the discovery of novel drug targets and biomarkers. The results obtained in this study will contribute to the understanding of the aging process and the prevention of accelerated aging and aging-associated diseases.

Tables and Figures

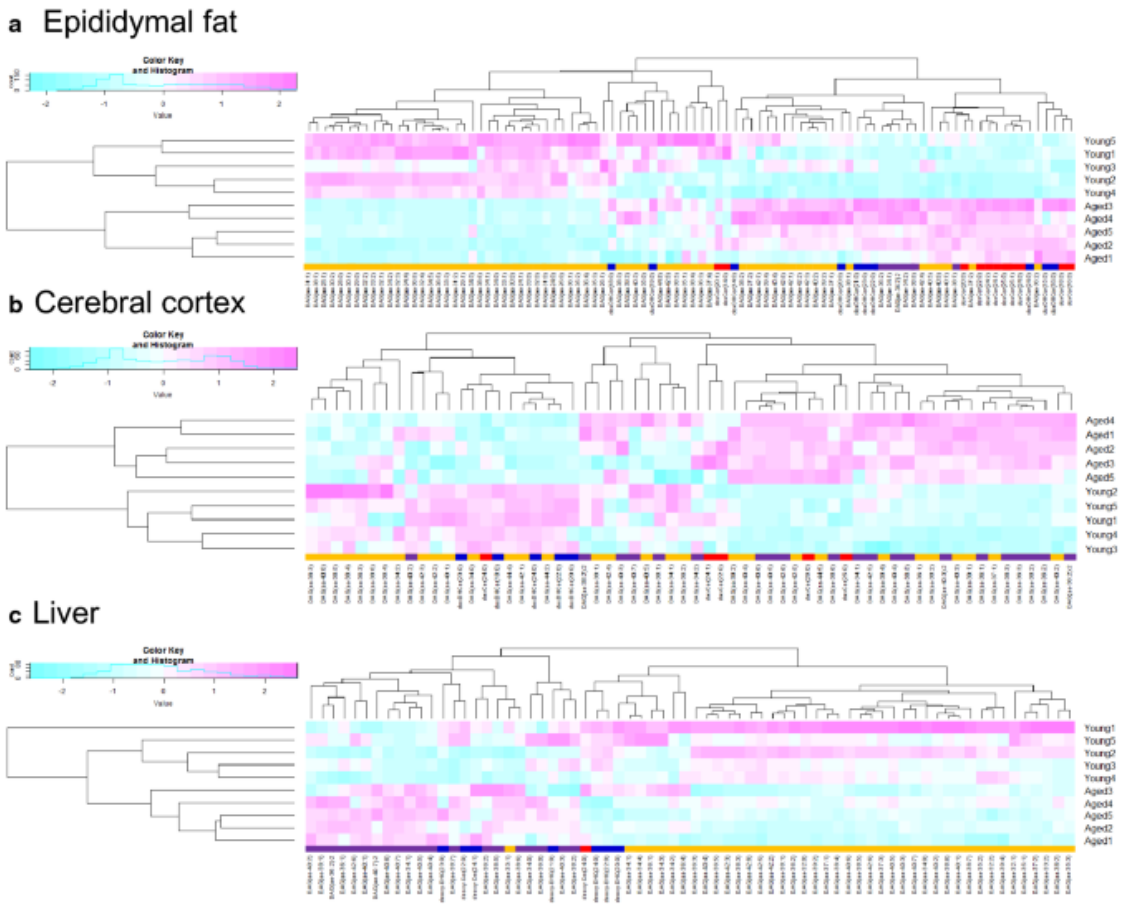

Fig. 1. Two-dimensional cluster heat-map visualization of detected lipids and metabolites from aged and young mice. DoxCers (red), doxDHCers (blue), DAG (aa) (yellow) and DAG (ae) (purple) in epididymal fat **(a)**, the cerebral cortex **(b)**, and the liver **(c)** in young (9 weeks old) and aged (114 weeks old) mice. DAG, diacylglycerol; aa, di-acyl; ae, acyl and ether; doxDHCer, deoxydihydroceramide; doxCer, deoxyceramide.

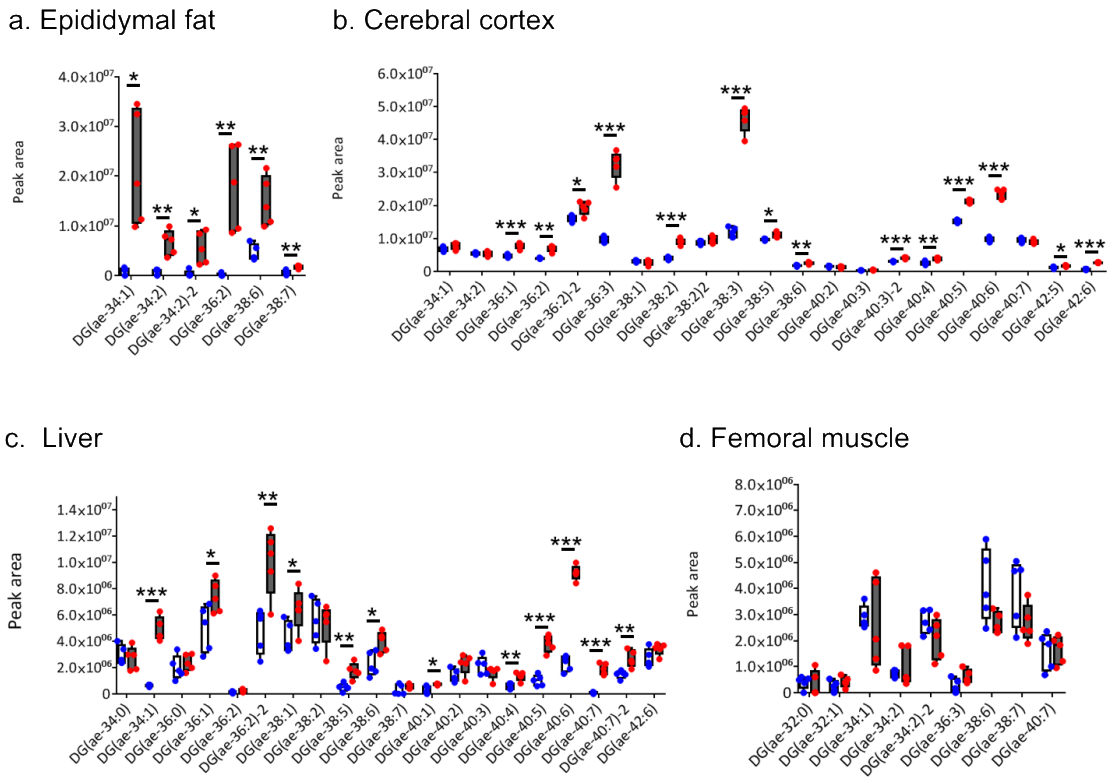

Fig 2. Integrated peak areas of Ether-linked DAGs across the organs. The ether-linked DAGs In epididymal fat **(a)**, the cerebral cortex **(b)**, liver **(c)**, and femoral muscle **(d)** in young and aged mice. Data are presented as box-and-whisker plot, with whiskers showing minimum and maximum values and each dot plot showing individual values (white bar and blue dot: young, gray bar and red dot: aged). p-values are indicated for the metabolites with significant differences in terms of abundance between groups. *$p < 0.05$, **$p < 0.01$, ***$p < 0.001$.

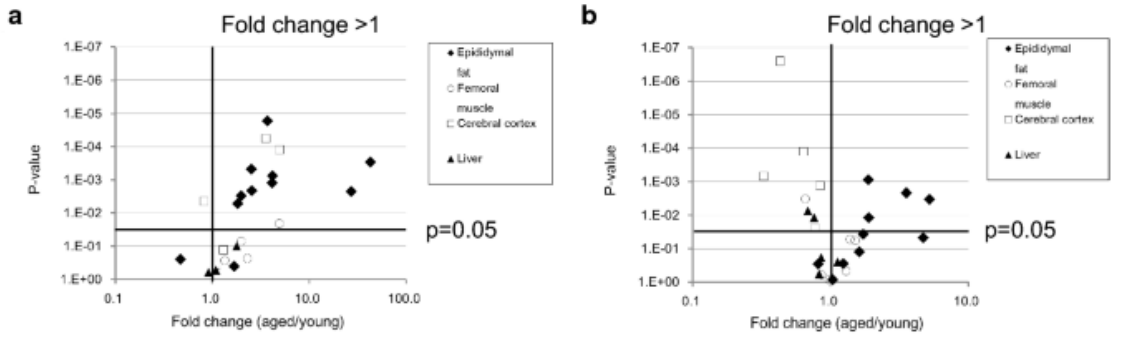

c

		Epididymal fat tissues			Femoral muscle			Cerebral cortex			Liver		
	Animal number	young	aged	Fold change (Aged/young)	young	aged	Fold change (Aged/young)	young	aged	Fold change (Aged/young)	young	aged	Fold change (Aged/young)
L-Ala (nmol/g)	#1	13.6	5.1	0.38	160.2	107.0	0.67	57.0	46.2	0.81	128.5	72.9	0.57
	#2	7.9	23.5	2.98	115.6	101.7	0.88	53.7	43.5	0.81	66.0	59.7	0.90
	#3	19.6	10.4	0.53	141.4	99.9	0.71	59.3	46.1	0.78	95.4	67.8	0.71
	#4	6.7	9.7	1.46	123.7	106.4	0.86	57.3	49.2	0.86	78.8	92.5	1.17
	#5	11.5	3.8	0.33	133.1	91.5	0.69	56.7	45.1	0.80	75.3	77.0	1.02
	Mean	11.9	10.5	1.14	134.8	101.3	0.76**	56.8	46.0	0.81***	88.8	74.0	0.88
	S.D.	5.1	7.8		17.2	6.3		2.0	2.1		24.6	12.2	
L-Ser (nmol/g)	#1	6.5	2.1	0.32	23.7	12.4	0.52	93.8	71.5	0.76	18.2	12.8	0.70
	#2	3.8	12.7	3.32	15.4	14.8	0.96	93.3	69.8	0.75	20.5	17.2	0.84
	#3	8.0	4.7	0.59	20.2	13.9	0.69	90.6	68.8	0.76	17.9	13.1	0.73
	#4	3.2	5.2	1.63	19.2	18.9	0.98	89.2	75.7	0.85	17.9	13.9	0.78
	#5	5.3	2.8	0.53	18.6	13.7	0.73	90.9	75.6	0.83	16.5	13.1	0.80
	Mean	5.4	5.5	1.28	19.4	14.7	0.78	91.6	72.3	0.79***	18.2	14.0	0.77**
	S.D.	2.0	4.2		3.0	2.5		1.9	3.2		1.5	1.8	
L-Ala/L-Ser	#1	2.1	2.4	1.17	6.8	8.7	1.28	0.6	0.6	1.06	7.0	5.7	0.81
	#2	2.1	1.8	0.90	7.5	6.9	0.91	0.6	0.6	1.08	3.2	3.5	1.08
	#3	2.4	2.2	0.90	7.0	7.2	1.03	0.7	0.7	1.02	5.3	5.2	0.97
	#4	2.1	1.9	0.89	6.4	5.6	0.88	0.6	0.6	1.01	4.4	6.7	1.51
	#5	2.2	1.4	0.62	7.1	6.7	0.94	0.6	0.6	0.96	4.6	5.9	1.28
	Mean	2.2	1.9	0.90	7.0	7.0	1.01	0.6	0.6	1.03	4.9	5.4	1.13
	S.D.	0.2	0.4		0.4	1.1		0.0	0.0		1.4	1.2	

Fig. 3. Volcano plot of the fold changes in the levels of doxSLs and concentrations of L-Ser and L-Ala. DoxCer **(a)** and doxDHCer **(b)** between aged and young mice and the corresponding p-values (white square: cerebral cortex; black triangle: liver; white circle: femoral muscle; black diamond: epididymal fat tissues). Each data point represents the mean value of five mice per group and different carbon chain-length and degree of unsaturation of fatty acid in each metabolite. A log 10 scale is used for the x-axis. **(c)** Fold changes (aged/young) in the mean concentrations of L-Ser and L-Ala. p-values are indicated for the metabolites with significant differences in abundance between groups. *$p < 0.05$, **$p < 0.01$, ***$p < 0.001$.

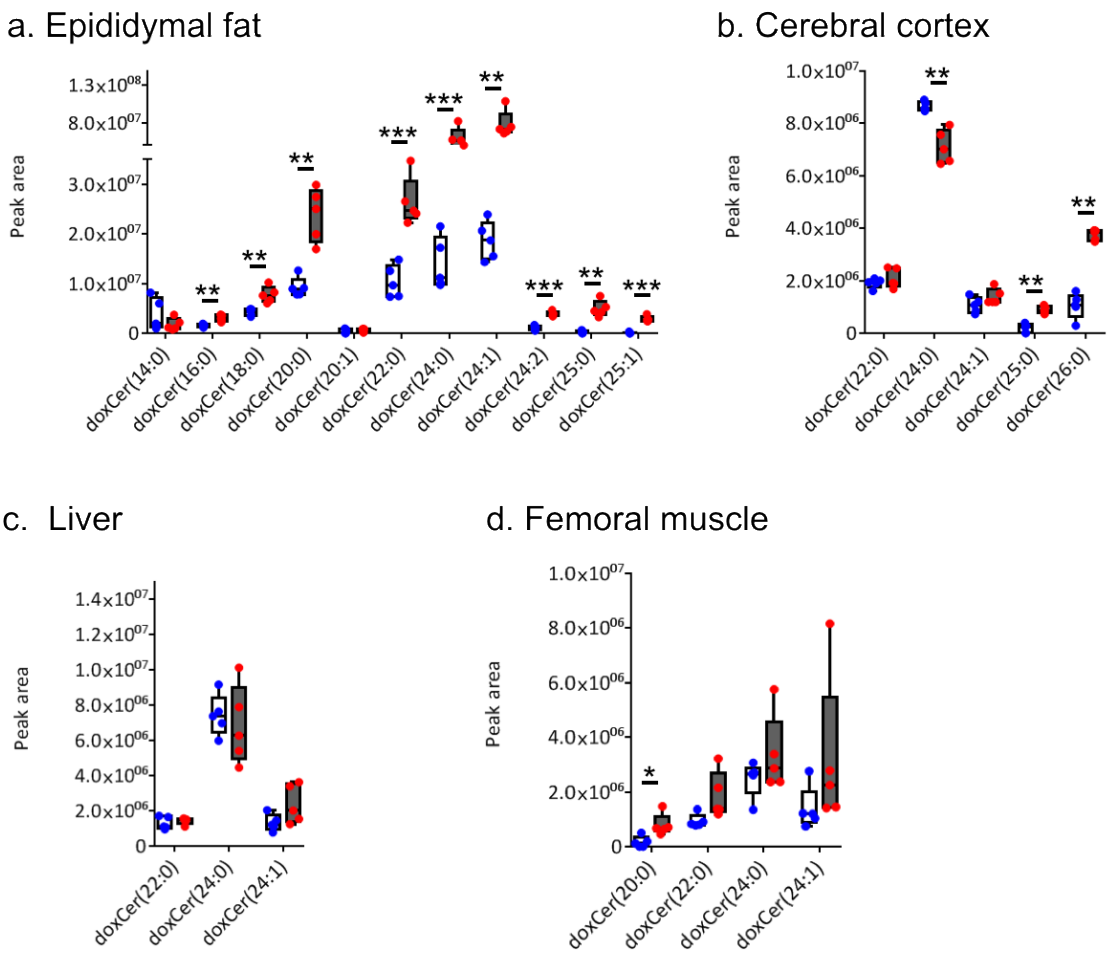

Fig 4. Integrated peak areas of doxCers across the organs. The doxCers in epididymal fat **(a)**, the cerebral cortex **(b)**, liver **(c)**, and femoral muscle **(d)** in young (9 weeks old) and aged (114 weeks old) mice. Data are presented as box-and-whisker plot, with whiskers showing minimum and maximum values and each dot plot showing individual values (white bar and blue dot: young, gray bar and red dot: aged). p-values are indicated for the metabolites with significant differences in terms of abundance between groups. Abbreviations: DG, diacylglycerol; ae, acyl and ether. *p < 0.05, **p < 0.01, ***p < 0.001.

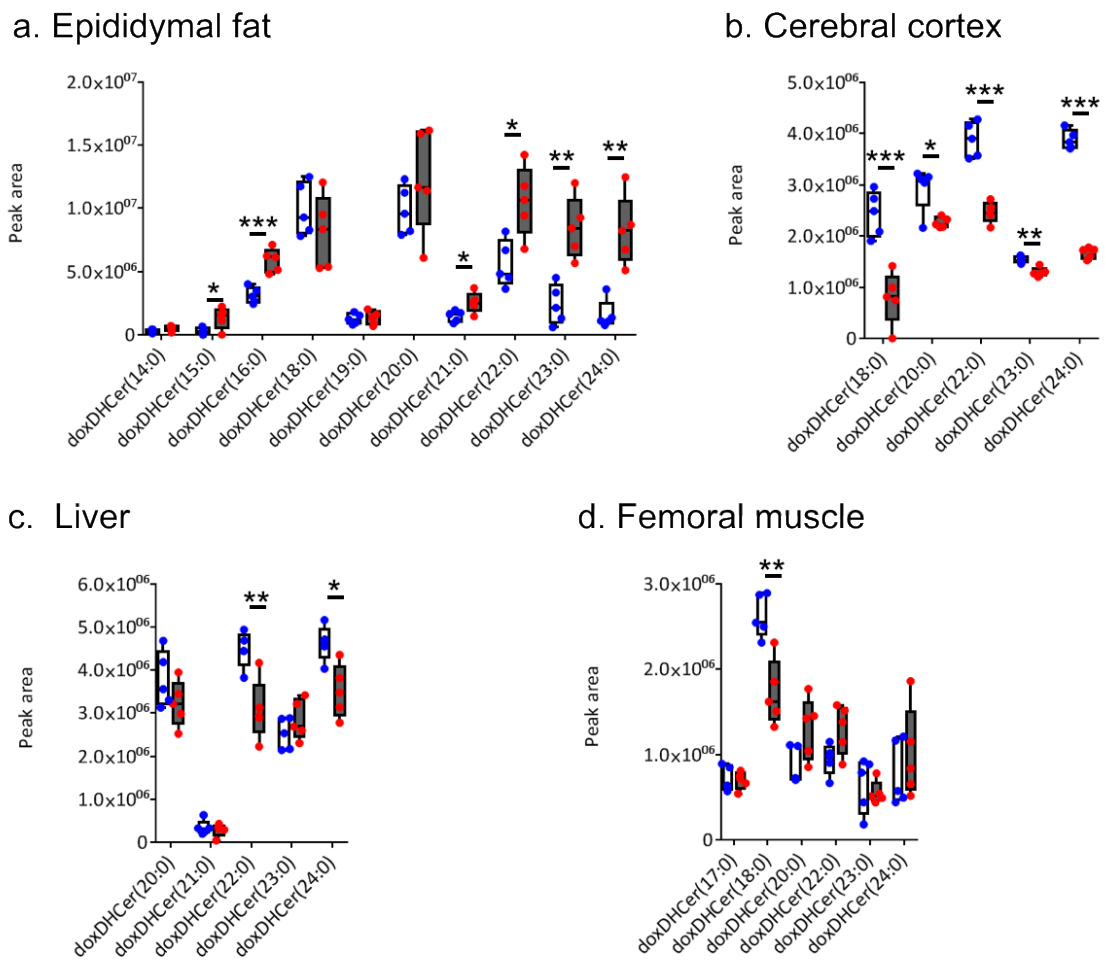

Fig 5. The doxDHCers in epididymal fat (a), the cerebral cortex (b), liver (c), and femoral muscle (d) in young (9 weeks old) and aged (114 weeks old) mice. Data are presented as box-and-whisker plot, with whiskers showing minimum and maximum values and each dot plot showing individual values (white bar and blue dot: young, gray bar and red dot: aged). p-values are indicated for the metabolites with significant differences in terms of abundance between groups. *p < 0.05, **p < 0.01, ***p < 0.001.

.

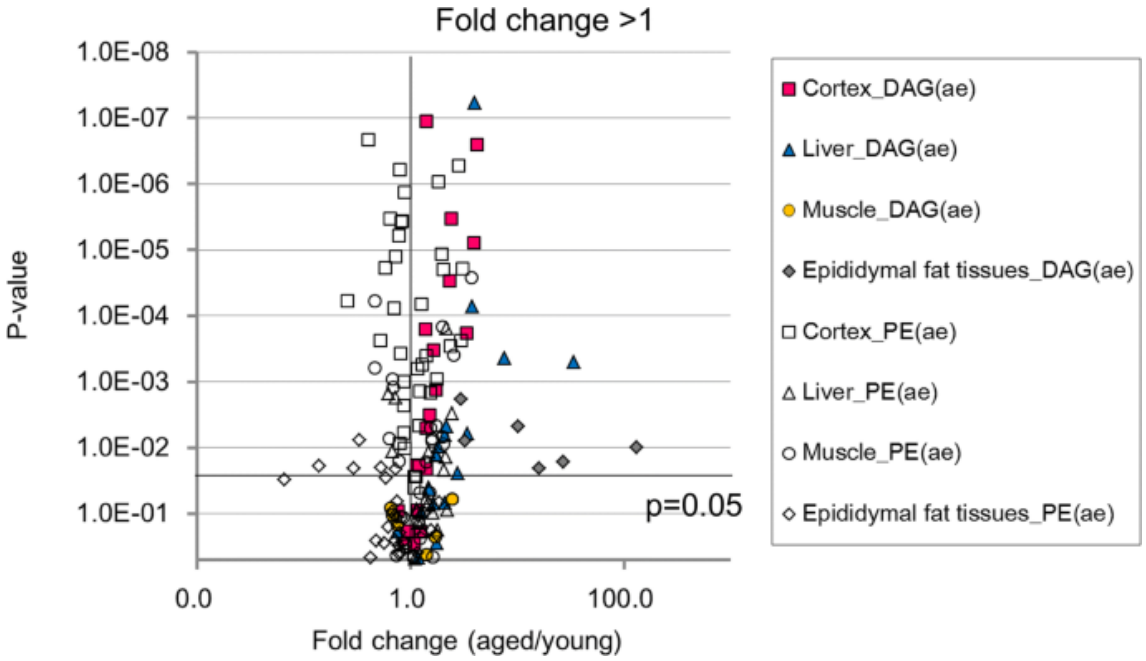

Fig. 6. Volcano plot of the fold changes in the levels of ether-linked diacylglycerols and ethanolamine plasmalogens. Ether-linked DAG (pink square: cerebral cortex; blue triangle: liver; yellow circle: femoral muscle; gray diamond: epididymal fat tissue) and ethanolamine plasmalogens (white square: cerebral cortex; white triangle: liver; white circle: femoral muscle; white diamond: epididymal fat tissues) between aged and young mice and the corresponding p-values. Each data point represents the mean value of five mice per group and different carbon chain-length and degree of unsaturation of fatty acid in each metabolite. A log 10 scale is used for the x-axis.

Table 1. Plasma biochemical parameters. Glucose (Glu), triglyceride (TG), glutamic pyruvic transaminase (GPT), total cholesterol (T-CHO), and total ketone body (T-KB) levels; body weights; and weight reduction rates (%).

		Glu (mg/dL)	TG (mg/dL)	GPT (U/L)	T-CHO (mg/dL)	T-KB (μmol/L)	Body weight (pre/fast (g))	Weight reduction rate (%)
mean.	aged	117.0	35.0	49.8	73.1	1433.9	37.4/34.3	91.8%
	young	140.0	40.6	26.8	85.4	2184.6	23.9/20.2	84.9%
S.D.	aged	17.9	32.2	25.6	9.3	221.2	2.3/2.6	2.0%
	young	13.3	8.9	4.6	13.0	329.1	1.1/0.9	1.1%
t-test		0.053	0.721	0.115	0.129	0.004	0.0006/0.083	

Chapter 2: A Simple and Highly Sensitive Quantitation of Eicosanoids in Biological Samples Using Nano-flow Liquid Chromatography/Mass Spectrometry

Abstract

A simple sample preparation method for eicosanoid was developed by the combination of deproteinization and nanoLC-ESI-MS/MS. Eicosanoids are a group of bioactive lipid mediators, present in trace amounts in the body. Therefore, an analytical method for eicosanoids requires superior sensitivity. The method described in this report, which takes advantage of the highly sensitive power of nanoLC-ESI-MS/MS, enabled a simplification of the sample-preparation process. Eicosanoid extraction was performed just by homogenization in methanol with subsequent phospholipid removal, and then the liquid phase was directly subjected to nanoLC-ESI-MS/MS analysis without a condensation process. The quantitation range achieved 0.01 - 100 ng/mL for thromboxane B_2, and 0.05 - 100 ng/mL for prostaglandin E_2, prostaglandin D_2, prostaglandin F_2, leukotriene B_4, 6-keto prostaglandin $F_{1\alpha}$ and 11-dehydro thromboxane B_2. Rat brain sample analyses demonstrated the feasibility of the quantification of those seven eicosanoids from biological samples.

Introduction

Eicosanoid is a family of bioactive lipids synthesized by the enzymatic oxidation of 20-carbon fatty acids, such as arachidonic acid, consisting of several sub-families; prostaglandins, prostacyclins, thromboxane, and leukotrienes. The variety of molecular species contributes to exerting diverse biological functions and regulating various body responses, such as inflammation, immune system regulation, muscle contraction, pain, and body temperature control (Bozza *et al.*, 2011; Calder, 2009; Dennis and Norris, 2015; Wanggren *et al.*, 2008; Trebino *et al.*, 2003; Narumiya *et al.*, 1998; Divangahi *et al.*, 2010). These functions are mostly derived from structural differences of the eicosanoids. Therefore, the simultaneous measurement of eicosanoids is valuable for understanding their physiological and pathophysiological roles.

In the past, eicosanoids were mainly analyzed by gas chromatography-mass spectrometry (GC/MS) (Balazy *et al.*, 1986; Liu *et al.*, 2009), enzyme-linked immunosorbent assays (ELISA)(Shono *et al.*, 1988; Reinke, 1992) and LC/MS/MS. The drawback of ELISA is being able to detect only a single analyte in a single set of analysis. As for GC/MS, the sensitivity and selectivity is great. However, they require chemical derivatization steps. As for LC/MS/MS analysis, previous reports indicated various analytical platforms. For example, liquid-liquid extraction for the determine eicosanoids in plasma with LC/MS/MS, (Ostermann *et al.*, 2015)plasma analysis using online-SPE-LC-MS/MS (Kortz *et al.*, 2013), by using a new atmospheric pressure ionization source to enhance the performance for eicosanoid analysis (Lubin *et al.*, 2016) and human plasma analysis using ultra-fast liquid chromatography (UFLC) for prostaglandins (Gachet *et al.*, 2015), endocannabinoids and steroids metabolites, and eicosanoids

analysis using ultra performance liquid chromatography (UPLC) for plasma sample (Wang *et al.*, 2016) and urine sample (Sasaki *et al.*, 2017) were reported.

For that purpose, LC/MS/MS has been used as a suitable technology that enables highly sensitive and simultaneous measurements; however, since the amount of eicosanoids contained in biological samples is extremely small, the analytical quality is significantly influenced by the pre-analytical sample preparation.

Pre-analytical sample preparation is regarded as being indispensable for sensitive and robust quantitation. Solid-phase extraction (SPE) with reverse phase (Ostermann *et al*., 2015; Takabatake *et al*., 2002; Wang *et al*., 2014), strong anion exchange, 20 and strong cation exchange (Dahl *et al*., 2008; Peterson *et al*., 2002) is a key method for the selective extraction and condensation of target molecules. Liquid-liquid extraction (LLE)(Ostermann *et al*., 2015; Rago *et al*., 2013) is also frequently used for metabolite fractionation by solvent partitioning and protein removal. These processes largely contribute to the enrichment of target molecules and the removal of abundant interferences, enabling efficient measurements of trace metabolites in combination with LC/MS/MS analysis. (Takabatake *et al*., 2002; Dahl *et al*., 2008). One successful application of this method is eicosanoid analysis (Kita *et al*., 2005). SPE and LLE are often applied to the sample preparation of eicosanoid analysis, enabling the detection of eicosanoids by raising the concentration above the detection limit; however, the multiple sample preparation processes are laborious and time-consuming tasks, and the data quality relies largely on skill and experience. These issues could be solved by robotic automation, but a more convenient approach would be desirable.

In this study, protein precipitation by a water-soluble organic solvent was evaluated as a method for simplified sample preparation for eicosanoid analysis by

utilizing nanoLC-ESI-MS/MS. NanoLC-ESI-MS/MS has been established, especially in the proteomics field, as the standard methodology for the quantitation and identification of small amounts of proteins (Peng *et al*., 2003; Ishihama *et al*., 2002; Licklider *et al*., 2002) because of its superior sensitivity compared to conventional LC/MS/MS. Recently, the technology has been expanded to small molecule analyses and metabolomics research, mostly for relatively abundant metabolites (Myint *et al*., 2009; Khin *et al*., 2009; Uehara *et al*., 2009). The highly sensitive power of nanoLC-ESI-MS/MS should also be beneficial for trace component analysis as well. I hypothesized that the sensitivity of nanoLC-ESI-MS/MS could compensate for the minimized sample preparation. This approach was validated to be an easy and quantitative method using rat brain samples.

Material and methods

Chemicals, reagents, and materials

Acetonitrile, isopropanol, methanol, acetone, acetic acid, and formic acid (all LC/MS grade) were purchased from Wako Pure Chemical (Osaka, Japan). Prostaglandin E_2 (PGE_2), prostaglandin D_2 (PGD_2), 6-keto prostaglandin $F_{1\alpha}$ (6-keto $PGF_{1\alpha}$), prostaglandin $F_{2\alpha}$ ($PGF_{2\alpha}$), leukotriene B_4 (LTB_4), thromboxane B2 (TXB_2), and 11-dehydro thromboxane B_2 (11-dehydro TXB_2) were purchased from Cayman Chemical Co., Ltd. (Ann Arbor, MI, USA). These reagents were dissolved in methanol, and standard mixture solutions were prepared at 0.1, 0.5, 1, 5, 10, 50, 100, 500, and 1,000 ng/mL. PGE_2-d_4, PGD_2-d_4, LTB_4-d_4, 6-keto $PGF_{1\alpha}$-d_4, $PGF_{2\alpha}$-d_4 TXB_2-d_4, and 11-dehydro TXB_2-d_4 were also purchased from Cayman Chemical Co., Ltd. These deuterium-labeled reagents were dissolved in methanol (10 ng/mL each) and used as internal standard (IS) solutions. Rat brain and plasma (Crl:CD, 8-week-old males) were purchased from Japan SLC, Inc. (Shizuoka, Japan). Charcoal stripped human EDTA plasma was purchased from BioChemed services (Winchester, VA). Fatty acid-free human serum albumin was purchased from Sigma-Aldrich (St. Louis, MO) and diluted with MilliQ water (4%, w/v). All of these standard solutions and samples were frozen at −80 °C until use.

Nano-flow LC/MS/MS condition

A Dionex Ultimate 3000 nano-flow liquid chromatography system (Thermo Fisher Scientific Inc.) which consists of a high-pressure binary pump, a column oven, and a 6-port switching valve was used for chromatographic separation. Monolithic columns were selected as trap (Monocap for fast flow, 100 mm × 50 μm i.d., Kyoto Monotech,

Kyoto, Japan) and separation columns (Monocap for nano flow, 300 mm × 50 μm i.d., Kyoto Monotech). The column temperature was maintained at 50°C. Samples were loaded onto the trap column using a loading pump with acetic acid/Milli-Q water (0.1/100, v/v) at a flow rate of 5 μL/min. After 10 min of trapping, the 6-port valve was switched to the separation mode, and a gradient elution was performed with 0.1% acetic acid in Milli-Q water (solvent A) and 0.1% acetic acid in acetonitrile:isopropanol:acetone (90:5:5, solvent B) at a flow rate of 200 nL/min. The gradient was used as follows (time, %B): 0 min, 2%; 10 min, 2%; 30 min, 25%; 50 min, 50%; 60 min, 98%; 75 min, 98%; 75.1 min, 2%; 85 min, 2%. The eluate from the separation column was directly introduced to a nano-electrospray needle (FS360-50-15-D, New Objective Inc., MA, USA) and ionized in negative ionization mode. The ion source conditions were set as follows: the spray voltage was 1,750 V, the heated-capillary temperature was 270°C, and the sheathe gas (N2) pressure was 30 psi. A TSQ Vantage triple quadrupole mass spectrometer (Thermo Fisher Scientific Inc.) was used for eicosanoid detection in a selected reaction monitoring mode (SRM). Eicosanoids mostly produce $[M-H]^-$ ion by negative ionization; thus, the $[M-H]^-$ ion was set as Q1. Q3 was selected based on the intensity and the specificity of the target molecules; however, there are some eicosanoids whose Q1/Q3 are the same because of their structural similarities; therefore, chromatographic separation is necessary to distinguish isomeric molecules, such as PGE2 and PGD2. Table 1 contains a list of the mass-spectrometry parameters for seven eicosanoids and deuterium-labeled internal standards whose chromatograms were acquired by the timed-SRM mode with a 2 min scheduled time window and a 1.5 sec cycle time. Mass resolutions for Q1 and Q3 were set at 0.7 Da full-width at the half-maximum (FWHF) for all molecules. The Xcalibur software package (Thermo Fisher

Scientific Inc.) was used for peak detection, integration, and quantitative calculations of the mass spectrometry data.

Sample preparation

Frozen brain tissue was weighed and transferred to a test tube in ice. To exclude any differences between individuals and brain regions, the experiments were carried out using one pooled homogenate. The tissue sample was homogenized in three volumes (v/w) of ice-cold formic acid:methanol (0.5:99.5) by a ball mill (Retsch GmbH, Haan, Germany). A 400 μL of sample was mixed with 10 μL of an IS solution, and then transferred to a Captiva ND Lipids 96-well plate followed by centrifugation at 2,000 *g* for 2 min. Finally, the filtrated sample was directly injected to the nanoLC-ESI-MS/MS for analysis. For recovery and spike tests, a certain amount of standard solution (0, 25, and 250 ng/mL) was spiked into pooled brain homogenate to make the added concentration to be 0, 2.5, and 25 ng/g tissue.

Extraction efficiency test

The extraction efficiency was evaluated with a deuterium-labeled standard spiked into plasma. A 50 μL aliquot of rat plasma was transferred to a test tube (2.0 mL) in ice and mixed with 5 μL of IS solution to achieve a final concentration of 10 ng/mL. The sample was homogenized with 150 μL of ice-cold formic acid:methanol (0.5:99.5) or 150 μL of ice-cold formic acid:acetonitrile (0.5:99.5). The sample was transferred to a Captiva ND Lipids 96-well plate (Agilent Technologies) for efficient removal of the proteins and phospholipids, followed by centrifugation at 2,000 g for 2 min. Then, 10 μL of flow trough was directly applied for LC/MS/MS analysis.

Quantitation method

Calibration standards were prepared by diluting the standard stock solutions in methanol to final concentrations of 0.01, 0.05, 0.1, 0.5, 1, 5, 10, 50, and 100 ng/mL for all molecules. Fifty microliters of methanol were transferred to a test tube (2.0 mL) in ice and mixed with 5 μL of IS solution, 5 μL of methanol, and 150 μL of ice-cold formic acid:methanol (0.5:99.5). The sample was vortex mixed for 1 min, and then all of the homogenate solution was transferred to a Captiva ND Lipids 96-well plate, followed by centrifugation at 2,000 *g* for 2 min. Finally, 10 μL of the flow trough was directly applied for LC/MS/MS analysis. The calibration curve was calculated by a least-square linear regression method with 1/x weighting. The quantitative accuracy and precision was evaluated by a standard solution prepared at three different concentrations (final concentration: 0.2, 2 and 20 ng/mL, n = 3).

Recovery rates

Recovery rates were determined by comparing the peak areas of deuterium-labeled standards that were added to the brain both before (pre-spiked) and after (post-spiked) sample preparation. Pre-spiked samples were prepared as follows: Deuterium-labeled standards were spiked in 50 μL of brain homogenate at 5 ng/mL, and then followed by the sample-preparation procedure described above. After extraction, 5 μL of methanol was added to the eluate. For post-spiked samples, deuterium labeled standards were added after sample preparation. The recovery rate was calculated as follows: Recovery rate (%) = (peak area of pre-spiked standard)/(peak area of post-spiked standard) × 100.

Results and Discussion

Chromatographic separation

Eicosanoid is a group of lipid mediator synthesized from arachidonic acid, called an arachidonic acid cascade, mainly consisting of 6 different bioactive molecules: PGE_2, PGD_2, $PGF_{2\alpha}$, PGI_2, TXA_2, and LTA_4. Some of them are quickly metabolized to stable forms in a body, such as 6-keto-$PGF_{1\alpha}$ from PGI_2, TXB_2 and 11-dehydroxy-TXB_2 from TXA_2, and LTB_4 from LTA_4, which can be indicators of each pathway. Therefore, seven eicosanoids (PGE_2, PGD_2, $PGF_{2\alpha}$, 6-keto-$PGF_{1\alpha}$, TXB_2, 11-dehydroxy-TXB_2 and LTB_4) were selected as target molecules for analytical evaluation in this study as indicators of inflammatory responses derived from arachidonic acid cascade.

The mass-spectrometry parameters of all the target analytes are listed in Table 1. PGE_2 and PGD_2 had the same Q1 and Q3 value, and the other parameters were also almost identical; therefore, mass spectrometry alone could not differentiate these two molecules. Figure 1 shows a nanoLC-ESI-MS/MS chromatogram of a standard mixture containing seven eicosanoids (25 pg on column). A monolith chromatographic column was selected for the nano-LC separation with an 85 min runtime, including a 10 min pre-concentration step. The chromatographic conditions enabled the separation of PGE_2 and PGD_2 at 42.2 min and 43.0 min respectively. A shoulder peak was observed in TXB_2 chromatogram. A similar chromatogram was reported in other article(Kita *et al*., 2005; Yu *et al*., 2011). I currently speculated that these peaks were derived from multi form TXB_2 with the equilibrium state.

The relative standard deviations (RSD) of the retention times of the analytes were all less than 0.2% (Table 1) and the RSD of the peak area of the deuterium labeled

standards were all less than 13.0% indicating the robustness of the chromatographic conditions (n = 16).

Sample preparation

Methanol or acetonitrile was generally used for a water-soluble organic solvent based protein precipitation; however, the extraction efficiency could be different depending on the molecule of interest. A comparison of the LC/MS/MS peak area between methanol extraction and acetonitrile extraction for stable isotope-labeled PGE_2, PGD_2, and LTB_4 spiked in rat plasma was conducted. PGE_2 and PGD_2 revealed no significant differences, whereas methanol exhibited a larger intensity for LTB_4 extraction (Fig. 2, sample preparation method is given in section Extraction efficiency test). This difference could be the result of both the extraction efficiency and the matrix effect derived from interferences in the extract. The lower extraction efficiency of LTB_4 in acetonitrile could be mainly derived from a combination of these two factors. The major cause was not identified in this study; however, based on comparison data, methanol was selected as a suitable solvent for sample preparation.

Recovery rates

The recovery rates in the sample preparation process and the analytical reproducibility of all target molecules were determined using stable isotope-labeled standards spiked into rat plasma. The recovery rates of all molecules were greater than 70% (Table. 2). The analytical reproducibility, evaluated by the relative standard deviation (RSD) of seven replicates, were all less than 15 %. In a previous report, the recovery rates of eicosanoid by LLE were 10.61 % for TXB_2, 25.56 % for 11-dehydroxy

TXB_2, 35.19 % for $PGF_{2\alpha}$, 33.21 % for PGD2, 49.19 % for PGE_2 and 12.75% for 6-keto $PGF_{1\alpha}$ extracted with two-step LLE (the first extraction was chloroform/isopropanol (2:1); the second extraction was with methyl tert-butyl ether)(Mangal, Uboh, and Soma 2011) and 22.1% for PGD_2, 26.5% for PGE2, 21.1% for LTB_4 and 29.5% for $PGF_{2\alpha}$ when extracted with 1M acetic acid/2-isopropanol/hexane (2:20:30, v/v/v) (Rago and Fu 201). As for the recovery rate of eicosanoid using a SPE column, more than 65% by weak anion-exchange, 0-54% by strong anion-exchange and more than 68% by octadecylsilyl based column was reported (Ostermann *et al*., 2015). On the other hand, the recovery rate of our result was shown to be equal or above that of the SPE and LLE method. Taken together, nanoLC-ESI-MS/MS detection coupled with methanol extraction, and phospholipid removal was demonstrated to be a robust, reliable method for quantitative analysis.

Quantitative validation

The quantification of the seven eicosanoids was carried out using calibration curves prepared from standard solutions and stable isotope labeled internal standards using methanol as the blank matrix. A suitable blank matrix for endogenous molecule quantitation is the same or equivalent biological matrix without the target analytes. I first tested two protein solutions, fatty acid free human serum albumin solution (4%) and charcoal stripped human plasma, but LTB_4 was detected in both (Fig. 3). Thus, methanol was selected as a blank matrix for the calibration curve because methanol was also used in the sample preparation.

A linear dynamic range from 0.01 to 100 ng/mL (50 fg to 500 pg on column) was achieved for TXB_2, and from 0.05 ng/mL to 100 ng/mL (250 fg to 500 pg on column)

for PGE_2, PGD_2, LTB_4, 6-keto$PGF_{1\alpha}$, 11-dehydroTXB_2, and $PGF_{2\alpha}$ and correlation coefficients of $r > 0.99$ were obtained for all analytes (Table 3). The sensitivity was almost equivalent to the detection limits reported in other articles: 0.3±0.1 pg on column for PGE_2 and PGD_2 (Myint *et al.*, 2009), 10 pg on column for PGD_2, 5 pg on column for $PGF_{2\alpha}$ and TXB_2, 50 pg on column for 6-keto $PGF_{1\alpha}$ (Masoodi and Nicolaou, 2006), and 4 pg on column for LTB_4(Lin *et al*., 2013). To evaluate the validity of the calibration curve, spike-and-recovery tests were performed. For this purpose, rat brain was selected as a typical difficult-to-treat matrix because of the richness in lipids and proteins, which makes sample preparation difficult for removing those abundant constituents. Therefore, brain was considered to be an appropriate matrix to demonstrate the feasibility of the new procedure. Rat brain was mixed with specific amounts of standards (0, 2.5 and 25 ng/g tissue), and applied to the quantitative analysis. As a result, all eicosanoids were observed from the rat brain within the calibration range. The quantitative robustness of this method was exemplified based on the accuracies of spiked concentrations of all eicosanoids, 82.2–117.6% and RSD values less than 15% (Table 4). Moreover, the endogenous concentration observed in this experiment was almost equivalent to the values in other reports (Ramadan *et al*., 2012). Taken together, this study demonstrated the feasibility of this method for sample preparation and quantitation.

Many previous reports stated that the precise and accurate analysis of eicosanoids *in vitro* and *in vivo* is challenging due to their low concentration and the existence of structural isomers, making specific detection difficult. In addition, the analytical procedures in those reports required laborious sample-preparation processes. In this study, a combination of protein precipitation, phospholipid removal, and nanoLC-ESI-MS/MS was confirmed to be an improved approach, especially in sample preparation.

The minimized sample-preparation process reduced the sample preparation time and contributed to the consistent and reproducible results. The accuracy and precision observed in the analysis of rat-brain samples exemplified the data quality. In this study, nanoLC-ESI-MS/MS required a long run time of 85 minutes for the chromatographic separation of PGD_2 and PGE_2. For practical situations, a shorter run time analysis is demanded; however, this study demonstrated that the enrichment process by SPE or LLE is not necessary, even for eicosanoid analysis. In summary, I demonstrated that a robust quantification of endogenous metabolites could be carried out by nanoLC-ESI-MS/MS with simple sample preparation, indicating that this approach can be expanded to other metabolites that require highly sensitive analysis.

Tables and Figures

Table 1. Mass spectrometry parameters and retention time of analytes and identical stable- isotope labeled analytes.

						RSD, %	
Name	Q1 *(m/z)*	Q3 *(m/z)*	Collision energy/ V	S-lens /V	RT/ min	RT/ min	Peak area
PGE_2	351.2	271.1	18	83	43	0.11	-
PGD_2	351.2	271.1	19	83	42.2	0.12	-
$PGF_{2\alpha}$	353.2	193.2	22	133	41.2	0.05	-
6-ketoPGF$_{1\alpha}$	369.2	163.2	27	109	36.3	0.08	-
TXB_2	369.1	169.1	18	85	39.9	0.09	-
11-dehydroTXB_2	367.1	161.1	18	112	42.5	0.06	-
LTB_4	335.1	195.1	18	80	51.1	0.06	-
PGE_2-d_4	355.2	275.2	18	83	43	0.12	9.7
PGD_2-d_4	355.2	275.2	19	83	42.1	0.14	12.2
$PGF_{2\alpha}$-d_4	357.2	197.2	22	133	41.2	0.05	5.7
6-ketoPGF$_{1\alpha}$-d_4	373.2	167.1	27	109	36.3	0.08	8.3
TXB_2-d_4	373.1	173.1	18	85	39.9	0.09	6.9
11-dehydroTXB_2-d_4	371.1	165.1	18	112	42.5	0.1	6.7
LTB_4-d_4	339.1	197.1	18	80	51	0.05	8

Data represents mean calculated from the result of 16 samples.

Table 2. Extraction recovery of eicosanoids from rat plasma

Analyte	Recovery, %	RSD, %
6-ketoPGF$_{1\alpha}$-d$_4$	84.8	13.4
PGE$_2$-d$_4$	75	3.4
Thromboxane B$_2$-d$_4$	70.2	2.5
PGF$_{2\alpha}$-d$_4$	73.3	2.7
PGD$_2$-d$_4$	77.2	1.5
11-dehydroTXB$_2$-d$_4$	72.7	0.8
Leukotriene B$_4$-d$_4$	74.8	2.5

Data represents mean calculated from the result of 3 samples.

Table 3. Calibration range of seven target analytes determined by the calibration curve.

Nominal concentration	TXB_2		PGE_2		PGD_2		LTB_4		6-keto$PGF_{1\alpha}$		11-dehydro TXB_2		$PGF_{2\alpha}$	
(ng/mL matrix)	Accuracy, %	ng/mL	Accuracy, %	ng/mL	Accuracy, %	ng/mL	Accuracy, %	ng/mL	Accuracy, %	ng/mL	Accuracy, %	ng/mL	Accuracy, %	ng/mL
0.01	114	0.01	-	-	-	-	-	-	-	-	-	-	-	-
0.05	106	0.05	83	0.04	111	0.06	99	0.05	92	0.05	100	0.05	106	0.05
0.1	97	0.1	110	0.11	84	0.08	83	0.08	99	0.1	91	0.09	119	0.12
0.5	95	0.47	106	0.53	103	0.51	95	0.47	102	0.51	98	0.49	100	0.5
1	92	0.92	102	1.02	100	1	101	1.01	102	1.02	102	1.02	110	1.1
5	91	4.54	102	5.09	113	5.67	106	5.32	103	5.14	104	5.18	88	4.42
10	101	10.13	98	9.79	112	11.17	111	11.08	103	10.29	102	10.18	101	10.13
50	104	52.2	99	49.34	103	51.57	100	50.11	99	49.67	100	50.07	107	53.26
100	98	98.23	101	100.73	97	96.66	99	98.52	100	99.87	100	99.57	97	97.08
Intercept	0.0004		0.0148		0.0144		0.0019		0.0042		0.0194		0.0247	
Slope	0.1278		0.2942		0.2103		0.2856		0.0924		0.1504		0.3325	
Correlation coefficient	0.9989		0.9999		0.9952		0.999		0.9999		0.9999		0.9977	
Curve fitting	Linear		Linear		Linear		Linear		Linear		Linear		Linear	
Weighting	1 / x		1 / x		1 / x		1 / x		1 / x		1 / x		1 / x	

Table 4. Accuracy and precision of the spike-and-recovery tests of whole rat brains

	Nominal concentration (ng/g of brain tissue)	#01	#02	#03	#04	Mean. (ng/g of brain tissue)	Accuracy, %	RSD, %
	0	4.4	3.57	4.15	3.7	3.95		9.8
PGE_2	2.5	7	6.67	5.99	6.67	6.58	105.1	6.5
	25	30.14	27.11	25.44	33.73	29.11	100.6	12.5
	0	34.8	37.31	35.22	37.55	36.22		3.9
PGD_2	2.5	39.14	35.83	40.3	40.39	38.92	107.8	5.5
	25	63.3	57.95	63.83	61.11	61.55	101.3	4.3
	0	7.77	7.9	7.7	7.66	7.75		1.3
$PGF_{2\alpha}$	2.5	8.73	10.03	9.47	11.01	9.81	82.2	9.8
	25	37.86	27.5	32.91	38.21	34.12	105.5	14.8
	0	9.17	8.84	8.85	9.35	9.05		2.8
6-ketoPGF$_{1\alpha}$	2.5	11.25	11.9	11.51	13.03	11.92	114.8	6.6
	25	34.11	31.14	34.55	37.7	34.37	101.3	7.8
	0	15.7	16.82	16.25	15.59	16.09		3.5
TXB_2	2.5	18.05	19.12	19.12	19.35	18.91	112.9	3.1
	25	41.72	44.87	43.84	43.82	43.56	109.9	3
	0	0.06	0.06	0.05	0.05	0.05		4.1
11-dehydroTXB$_2$	2.5	2.9	3.47	2.6	2.99	2.99	117.5	12
	25	25.65	28.4	28.22	28.68	27.74	110.7	5.1
	0	0.09	0.08	0.07	0.08	0.08		7.8
LTB_4	2.5	2.96	2.99	3.2	2.94	3.02	117.6	4.1
	25	23.47	27.18	26.13	27.15	25.99	103.6	6.7

The standard solution was spiked into pooled brain homogenate to make the added concentration to be 0, 2.5, and 25 ng/g tissue. Data represents mean calculated from the result of 4 samples.

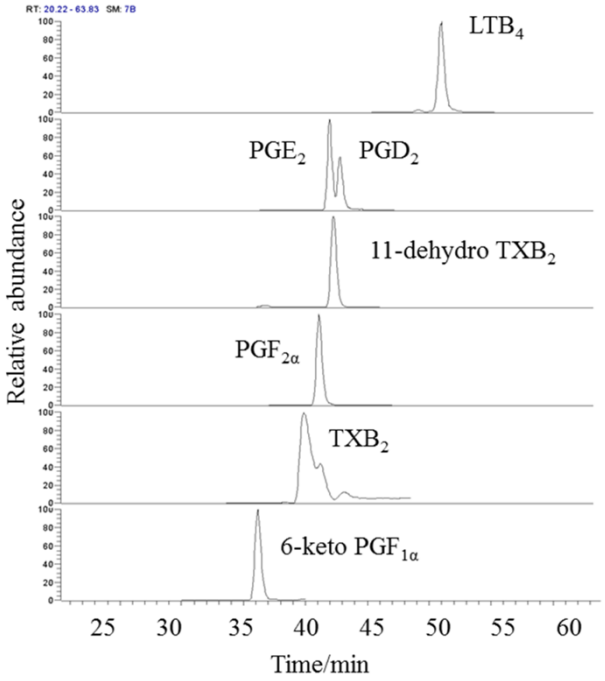

Fig. 1. Typical nanoLC-ESI-MS/MS chromatogram of seven eicosanoids. A standard mixture containing seven eicosanoids was applied to the column (25 pg of standard solution on column). Monocap for nano flow (300 mm × 50 μm, Kyoto Monotech.) was used as the separation column.

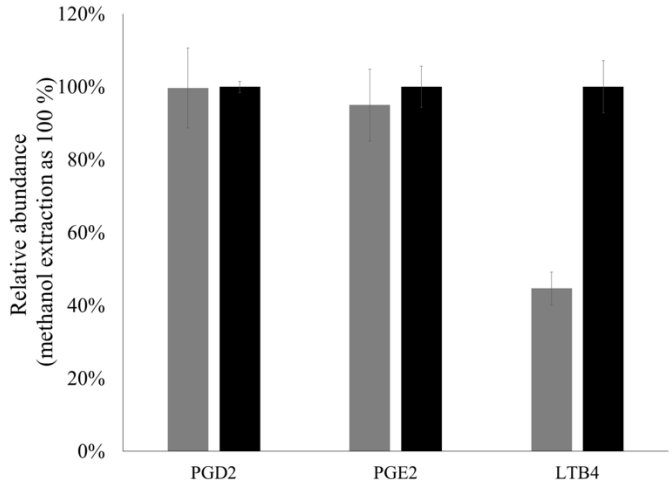

Fig. 2. Comparison of methanol extraction and acetonitrile extraction for stable isotope-labeled PGE_2, PGD_2, and LTB_4 spiked in rat plasma. Methanol extraction (gray bar) and acetonitrile extraction (black bar)). The data represents the mean calculated from the result of 3 samples.

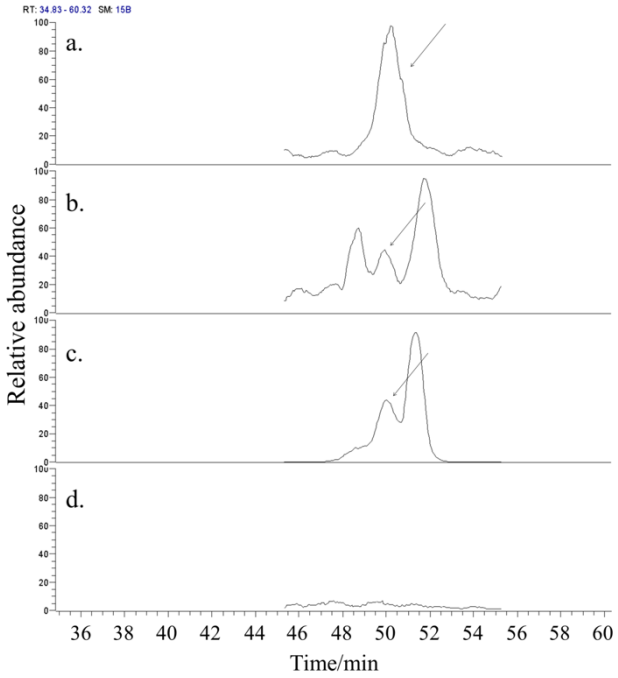

Fig. 3. The chromatogram of standard reagent (LTB_4), two protein solutions, organic solvent. The chromatogram of (**a)** deuterium labeled LTB_4, (**b)** extract of charcoal stripped human serum albumin, (**c)** extract of fatty acid free albumin, and (**d)** methanol. Each black arrow in the figure indicates the peak of LTB_4.

Acknowledgements

I am deeply grateful to Prof. Nakada, Prof. Tomiki Chiba, Prof. Ken-ichiro Ishida, and Asst. Prof. Kaori Ishikawa from University Tsukuba, for guiding my work and valuable discussions through my doctoral program.

I am very thankful to Mr. Masahiro Oka, Dr. Yoshinori Satomi, and Dr. Masaki Hosoya from Takeda Pharmaceutical Company Limited, for guiding my work and valuable discussions through my work.

I appreciate Dr. Toshiya Moriwaki, Dr. Hideki Hirabayashi, Dr.Hiroyuki Kobayashi, and Masaaki Kakehi, DVM from Takeda Pharmaceutical Company Limited, for their helpful supports.

I appreciate Dr. Satoru Hayashi, Dr. Kae Matsuda, Dr. Fuminari Yamaguchi, Mr. Yoshitaka Yasuhara, Ms. Mariko Miyabayashi, Mr. Taku Sugita, Ms. Megumi Hirayama, and Mrs. Chisato Takahara from Takeda Pharmaceutical Company Limited, for their technical supports.

Finally, I would like to appreciate my family, Dr. Tatsuya Ando and Miss Hana Ando, for supporting my life in University of Tsukuba.

References

Balazy, Michael., and Robert C. Murphy. 1986. “Determination of Sulfidopeptide Leukotrienes in Biological Fluids by Gas Chromatography Mass Spectrometry.” *Analytical Chemistry* 58(6):1098–1101.

Belsky, Daniel W., Avshalom Caspi, Renate Houts, Harvey J. Cohen, David L. Corcoran, Andrea Danese, HonaLee Harrington, Salomon Israel, Morgan E. Levine, Jonathan D. Schaefer, Karen Sugden, Ben Williams, Anatoli I. Yashin, Richie Poulton, and Terrie E. Moffitt. 2015. “Quantification of Biological Aging in Young Adults.” *Proceedings of the National Academy of Sciences* 112(30):E4104–10.

Benjamin, Daniel I., Alyssa Cozzo, Xiaodan Ji, Lindsay S. Roberts, Sharon M. Louie, Melinda M. Mulvihill, Kunxin Luo, and Daniel K. Nomura. 2013. “Ether Lipid Generating Enzyme AGPS Alters the Balance of Structural and Signaling Lipids to Fuel Cancer Pathogenicity.” *Proceedings of the National Academy of Sciences of the United States of America* 110(37):14912–17.

Bertea, Mariana, Markus F. Rütti, Alaa Othman, Jaqueline Marti-Jaun, Martin Hersberger, Arnold von Eckardstein, and Thorsten Hornemann. 2010. “Deoxysphingoid Bases as Plasma Markers in Diabetes Mellitus.” *Lipids in Health and Disease* 9(1):84.

Bozza, Patricia T., Ilka Bakker-Abreu, Roberta A. Navarro-Xavier, and Christianne Bandeira-Melo. 2011. “Lipid Body Function in Eicosanoid Synthesis: An Update.” *Prostaglandins Leukotrienes and Essential Fatty Acids* 85(5):205–13.

Braun, Fabian, Markus M. Rinschen, Valerie Bartels, Peter Frommolt, Bianca Habermann, Jan H. J. Hoeijmakers, Björn Schumacher, Martijn E. T. Dollé,

Roman-Ulrich Müller, Thomas Benzing, Bernhard Schermer, and Christine E. Kurschat. 2016. “Altered Lipid Metabolism in the Aging Kidney Identified by Three Layered Omic Analysis.” *Aging* 8(3):441–57.

Calder, Philip C. 2009. “Polyunsaturated Fatty Acids and Inflammatory Processes: New Twists in an Old Tale.” *Biochimie* 91(6):791–95.

Dahl, Sandra Rinne, Charlotte Ramstad Kleiveland, Moustapha Kassem, Tor Lea, Elsa Lundanes, and Tyge Greibrokk. 2008. “Detecting PM Concentrations of Prostaglandins in Cell Culture Supernatants by Capillary SCX-LC-MS/MS.” *Journal of Separation Science* 31(14):2627–33.

Dennis, Edward a., and Paul C. Norris. 2015. “Eicosanoid Storm in Infection and Inflammation.” *Nature Reviews Immunology* 15(8):511–23.

Divangahi, Maziar, Danielle Desjardins, Cláudio Nunes-Alves, Heinz G. Remold, and Samuel M. Behar. 2010. “Eicosanoid Pathways Regulate Adaptive Immunity to Mycobacterium Tuberculosis.” *Nature Immunology* 11(8):751–58.

Esaki, Kayoko, Tomoko Sayano, Chiaki Sonoda, Takumi Akagi, Takeshi Suzuki, Takuya Ogawa, Masahiro Okamoto, Takeo Yoshikawa, Yoshio Hirabayashi, and Shigeki Furuya. 2015. “L-Serine Deficiency Elicits Intracellular Accumulation of Cytotoxic Deoxysphingolipids and Lipid Body Formation.” *Journal of Biological Chemistry* 290(23):14595–609.

Farooqui, Akhlaq A., and Lloyd A. Horrocks. 2001. “Book Review: Plasmalogens: Workhorse Lipids of Membranes in Normal and Injured Neurons and Glia.” *The Neuroscientist* 7(3):232–45.

Ferreira, C. R., S. M. I. Goorden, A. Soldatos, H. M. Byers, J. M. M. Ghauharali-van der Vlugt, F. S. Beers-Stet, C. Groden, C. D. van Karnebeek, W. A. Gahl, F. M.

Vaz, X. Jiang, and H. J. Vernon. 2018. “Deoxysphingolipid Precursors Indicate Abnormal Sphingolipid Metabolism in Individuals with Primary and Secondary Disturbances of Serine Availability.” *Molecular Genetics and Metabolism* 124(3):204–9.

Gachet, María Salomé, Peter Rhyn, Oliver G. Bosch, Boris B. Quednow, and Jürg Gertsch. 2015. “A Quantitiative LC-MS/MS Method for the Measurement of Arachidonic Acid, Prostanoids, Endocannabinoids, N-Acylethanolamines and Steroids in Human Plasma.” *Journal of Chromatography. B, Analytical Technologies in the Biomedical and Life Sciences* 976–977:6–18.

Ginsberg, Lionel, Samina Rafique, John H. Xuereb, Stanley I. Rapoport, and Norman L. Gershfeld. 1995. “Disease and Anatomic Specificity of Ethanolamine Plasmalogen Deficiency in Alzheimer’s Disease Brain.” *Brain Research* 698(1–2):223–26.

Houck, Kristy L., Todd E. Fox, Lakshman Sandirasegarane, and Mark Kester. 2008. “Ether-Linked Diglycerides Inhibit Vascular Smooth Muscle Cell Growth via Decreased MAPK and PI3K/Akt Signaling.” *American Journal of Physiology. Heart and Circulatory Physiology* 295(4):H1657-68.

Houtkooper, Riekelt H., Carmen Argmann, Sander M. Houten, Carles Cantó, Ellen H. Jeninga, Pénélope A. Andreux, Charles Thomas, Raphaël Doenlen, Kristina Schoonjans, and Johan Auwerx. 2011. “The Metabolic Footprint of Aging in Mice.” *Scientific Reports* 1:134.

Ishihama, Yasushi, Juri Rappsilber, Jens S. Andersen, and Matthias Mann. 2002. “Microcolumns with Self-Assembled Particle Frits for Proteomics.” *Journal of Chromatography. A* 979(1–2):233–39.

Khin, Than Myint, Taisuke Uehara, Ken Aoshima, and Yoshiya Oda. 2009. “Polar Anionic Metabolome Analysis by Nano-LC/MS with a M*et al* Chelating Agent.” *Analytical Chemistry* 81(18):7766–72.

Kita, Yoshihiro, Toshie Takahashi, Naonori Uozumi, and Takao Shimizu. 2005. “A Multiplex Quantitation Method for Eicosanoids and Platelet-Activating Factor Using Column-Switching Reversed-Phase Liquid Chromatography-Tandem Mass Spectrometry.” *Analytical Biochemistry* 342(1):134–43.

Kortz, Linda, Juliane Dorow, Susen Becker, Joachim Thiery, and Uta Ceglarek. 2013. “Fast Liquid Chromatography–Quadrupole Linear Ion Trap-Mass Spectrometry Analysis of Polyunsaturated Fatty Acids and Eicosanoids in Human Plasma.” *Journal of Chromatography B* 927:209–13.

Kramer, Rita, Jacek Bielawski, Emily Kistner-Griffin, Alaa Othman, Irina Alecu, Daniela Ernst, Drew Kornhauser, Thorsten Hornemann, and Stefka Spassieva. 2015. “Neurotoxic 1-Deoxysphingolipids and Paclitaxel-Induced Peripheral Neuropathy.” *The FASEB Journal* 29(11):4461–72.

Latchoumycandane, Calivarathan, Laura E. Nagy, and Thomas M. McIntyre. 2015. “Myeloperoxidase Formation of PAF Receptor Ligands Induces PAF Receptor-Dependent Kidney Injury during Ethanol Consumption.” *Free Radical Biology and Medicine* 86:179–90.

Licklider, Lawrence J., Carson C. Thoreen, Junmin Peng, and Steven P. Gygi. 2002. “Automation of Nanoscale Microcapillary Liquid Chromatography-Tandem Mass Spectrometry with a Vented Column.” *Analytical Chemistry* 74(13):3076–83.

Lin, Weisheng, Mike-Qingtao Huang, Xiaohua Xue, Kirk Bertelsen, Guiyan Chen, Harry Zhao, Zhongping (John) Lin, Anne Fourie, Jan de Jong, and Naidong Weng.

2013. “A Highly Sensitive and Selective Method for the Determination of Leukotriene B4 (LTB4) in Ex Vivo Stimulated Human Plasma by Ultra Fast Liquid Chromatography–Tandem Mass Spectrometry.” *Journal of Chromatography B* 925:54–62.

Liu, Wei, Jason D. Morrow, and Huiyong Yin. 2009. “Quantification of F2-Isoprostanes as a Reliable Index of Oxidative Stress *in Vivo* Using Gas Chromatography–Mass Spectrometry (GC-MS) Method.” *Free Radical Biology and Medicine* 47(8):1101–7.

López-Otín, Carlos, Maria A. Blasco, Linda Partridge, Manuel Serrano, and Guido Kroemer. 2013. “The Hallmarks of Aging.” *Cell* 153(6):1194–1217.

Lubin, Arnaud, Suzy Geerinckx, Steve Bajic, Deirdre Cabooter, Patrick Augustijns, Filip Cuyckens, and Rob J. Vreeken. 2016. “Enhanced Performance for the Analysis of Prostaglandins and Thromboxanes by Liquid Chromatography-Tandem Mass Spectrometry Using a New Atmospheric Pressure Ionization Source.” *Journal of Chromatography A* 1440:260–65.

Mangal, Dipti, Cornelius E. Uboh, and Lawrence R. Soma. 2011. “Analysis of Bioactive Eicosanoids in Equine Plasma by Stable Isotope Dilution Reversed-Phase Liquid Chromatography/Multiple Reaction Monitoring Mass Spectrometry.” *Rapid Communications in Mass Spectrometry* 25(5):585–98.

Masoodi, Mojgan, and Anna Nicolaou. 2006. “Lipidomic Analysis of Twenty-Seven Prostanoids and Isoprostanes by Liquid Chromatography/Electrospray Tandem Mass Spectrometry.” *Rapid Communications in Mass Spectrometry : RCM* 20(20):3023–29.

Musial, A., A. Mandal, E. Coroneos, and M. Kester. 1995. “Interleukin-1 and Endothelin Stimulate Distinct Species of Diglycerides That Differentially Regulate Protein Kinase C in Mesangial Cells.” *The Journal of Biological Chemistry* 270(37):21632–38.

Myint, Khin Than, Ken Aoshima, Satoshi Tanaka, Tatsuji Nakamura, and Yoshiya Oda. 2009. “Quantitative Profiling of Polar Cationic Metabolites in Human Cerebrospinal Fluid by Reversed-Phase Nanoliquid Chromatography/Mass Spectrometry.” *Analytical Chemistry* 81(3):1121–29.

Nagan, N., and R. A. Zoeller. 2001. “Plasmalogens: Biosynthesis and Functions.” *Progress in Lipid Research* 40(3):199–229.

Narumiya, Shuh, Fumitaka Ushikubi, Eri Segi, Yukihiko Sugimoto, Takahiko Murata, Toshiyuki Matsuoka, Takuya Kobayashi, Hiroko Hizaki, Kazuhito Tuboi, Masato Katsuyama, Atsushi Ichikawa, Takashi Tanaka, and Nobuaki Yoshida. 1998. “Impaired Febrile Response in Mice Lacking the Prostaglandin E Receptor Subtype EP3.” *Nature* 395(6699):281–84.

Ostermann, Annika I., Ina Willenberg, and Nils Helge Schebb. 2015. “Comparison of Sample Preparation Methods for the Quantitative Analysis of Eicosanoids and Other Oxylipins in Plasma by Means of LC-MS/MS.” *Analytical and Bioanalytical Chemistry* 407(5):1403–14.

Peng, Junmin, Joshua E. Elias, Carson C. Thoreen, Larry J. Licklider, and Steven P. Gygi. 2003. “Evaluation of Multidimensional Chromatography Coupled with Tandem Mass Spectrometry (LC/LC−MS/MS) for Large-Scale Protein Analysis: The Yeast Proteome.” *Journal of Proteome Research* 2(1):43–50.

Penno, Anke, Mary M. Reilly, Henry Houlden, Matilde Laurá, Katharina Rentsch, Vera Niederkofler, Esther T. Stoeckli, Garth Nicholson, Florian Eichler, Robert H. Brown, Arnold von Eckardstein, and Thorsten Hornemann. 2010. "Hereditary Sensory Neuropathy Type 1 Is Caused by the Accumulation of Two Neurotoxic Sphingolipids." *Journal of Biological Chemistry* 285(15):11178–87.

Peterson, Zlatuse D., David C. Collins, Christopher R. Bowerbank, Milton L. Lee, and Steven W. Graves. 2002. "Determination of Catecholamines and Metanephrines in Urine by Capillary Electrophoresis-Electrospray Ionization-Time-of-Flight Mass Spectrometry." *Journal of Chromatography. B, Analytical Technologies in the Biomedical and Life Sciences* 776(2):221–29.

Petrosillo, G., M. Matera, G. Casanova, F. M. M. Ruggiero, and G. Paradies. 2008. "Mitochondrial Dysfunction in Rat Brain with Aging Involvement of Complex I, Reactive Oxygen Species and Cardiolipin." *Neurochemistry International* 53(5):126–31.

Rago, Brian, and Cexiong Fu. 2013. "Development of a High-Throughput Ultra Performance Liquid Chromatography-Mass Spectrometry Assay to Profile 18 Eicosanoids as Exploratory Biomarkers for Atherosclerotic Diseases." *Journal of Chromatography. B, Analytical Technologies in the Biomedical and Life Sciences* 936:25–32.

Ramadan, Epolia, Mireille Basselin, Jagadeesh S. Rao, Lisa Chang, Mei Chen, Kaizong Ma, and Stanley I. Rapoport. 2012. "Lamotrigine Blocks NMDA Receptor-Initiated Arachidonic Acid Signalling in Rat Brain: Implications for Its Efficacy in Bipolar Disorder." *The International Journal of Neuropsychopharmacology /*

Official Scientific Journal of the Collegium Internationale Neuropsychopharmacologicum (CINP) 15(7):931–43.

Reinke, M. 1992. “Monitoring Thromboxane in Body Fluids: A Specific ELISA for 11-Dehydrothromboxane B2 Using a Monoclonal Antibody.” *The American Journal of Physiology* 262(5 Pt 1):E658-62.

Sasaki Ai, Fukuda Hayato, Shiida Narumi, Tanaka Nobuaki, Furugen Ayako, Ogura Jiro, Shuto Satoshi, Mano Nariyasu & Yamaguchi Hiroaki. 2015." Determination of ω-6 and ω-3 PUFA metabolites in human urine samples using UPLC/MS/MS." *Analytical and Bioanalytical Chemistry* 407:1625–1639

Satomi, Yoshinori, Megumi Hirayama, and Hiroyuki Kobayashi. 2017. “One-Step Lipid Extraction for Plasma Lipidomics Analysis by Liquid Chromatography Mass Spectrometry.” *Journal of Chromatography B* 1063:93–100.

Seo, Chan, Yun-Ho Hwang, Youngbae Kim, Bo Sun Joo, Sung-Tae Yee, Cheol Min Kim, and Man-Jeong Paik. 2016. “Metabolomic Study of Aging in Mouse Plasma by Gas Chromatography–Mass Spectrometry.” *Journal of Chromatography B* 1025:1–6.

Shevchenko, Andrej, and Kai Simons. 2010. “Lipidomics: Coming to Grips with Lipid Diversity.” *Nature Reviews Molecular Cell Biology* 11(8):593–98.

Shono, Fumiaki, Kazushige Yokota, Kazumi Horie, Shozo Yamamoto, Kouwa Yamashita, Keiko Watanabe, and Hiroshi Miyazaki. 1988. “A Heterologous Enzyme Immunoassay of Prostaglandin E2 Using a Stable Enzyme-Labeled Hapten Mimic.” *Analytical Biochemistry* 168(2):284–91.

Takabatake, M., T. Hishinuma, N. Suzuki, S. Chiba, H. Tsukamoto, H. Nakamura, T. Saga, Y. Tomioka, A. Kurose, T. Sawai, and M. Mizugaki. 2002. “Simultaneous

Quantification of Prostaglandins in Human Synovial Cell-Cultured Medium Using Liquid Chromatography/Tandem Mass Spectrometry." *Prostaglandins, Leukotrienes, and Essential Fatty Acids* 67(1):51–56.

Trebino, C. E., J. L. Stock, C. P. Gibbons, B. M. Naiman, T. S. Wachtmann, J. P. Umland, K. Pandher, J. M. Lapointe, S. Saha, M. L. Roach, D. Carter, N. A. Thomas, B. A. Durtschi, J. D. McNeish, J. E. Hambor, P. J. Jakobsson, T. J. Carty, J. R. Perez, and L. P. Audoly. 2003. "Impaired Inflammatory and Pain Responses in Mice Lacking an Inducible Prostaglandin E Synthase." *Proceedings of the National Academy of Sciences* 100(15):9044–49.

Tu, Jia, Yandong Yin, Meimei Xu, Ruohong Wang, and Zheng-Jiang Zhu. 2017. "Absolute Quantitative Lipidomics Reveals Lipidome-Wide Alterations in Aging Brain." *Metabolomics : Official Journal of the Metabolomic Society* 14(1):5.

Uehara, Taisuke, Akira Yokoi, Ken Aoshima, Satoshi Tanaka, Tadashi Kadowaki, Masayuki Tanaka, and Yoshiya Oda. 2009. "Quantitative Phosphorus Metabolomics Using Nanoflow Liquid Chromatography-Tandem Mass Spectrometry and Culture-Derived Comprehensive Global Internal Standards." *Analytical Chemistry* 81(10):3836–42.

Wang, Nannan, Ronghua Dai, Weihui Wang, Yan Peng, Xiaoning Zhao, and Kaishun Bi. 2016. "Simultaneous Profiling of Eicosanoid Metabolome in Plasma by UPLC–MS/MS Method: Application to Identify Potential Makers for Rheumatoid Arthritis." *Talanta* 161:157–64.

Wang, Yan, Aaron M. Armando, Oswald Quehenberger, Chao Yan, and Edward A. Dennis. 2014. "Comprehensive Ultra-Performance Liquid Chromatographic

Separation and Mass Spectrometric Analysis of Eicosanoid Metabolites in Human Samples." *Journal of Chromatography. A* 1359:60–69.

Wanggren, K., A. Stavreus-Evers, C. Olsson, E. Andersson, and K. Gemzell-Danielsson. 2008. "Regulation of Muscular Contractions in the Human Fallopian Tube through Prostaglandins and Progestagens." *Human Reproduction* 23(10):2359–68.

Yang, Kui, Christopher M. Jenkins, Beverly Dilthey, and Richard W. Gross. 2015. "Multidimensional Mass Spectrometry-Based Shotgun Lipidomics Analysis of Vinyl Ether Diglycerides." *Analytical and Bioanalytical Chemistry* 407(17):5199–5210.

Yu, Rui, Lei Xiao, Guiqing Zhao, John W. Christman, and Richard B. van Breemen. 2011. "Competitive Enzymatic Interactions Determine the Relative Amounts of Prostaglandins E2 and D2." *Journal of Pharmacology and Experimental Therapeutics* 339(2):716–25.

Yuan, Min, Susanne B. Breitkopf, Xuemei Yang, and John M. Asara. 2012. "A Positive/Negative Ion-Switching, Targeted Mass Spectrometry-Based Metabolomics Platform for Bodily Fluids, Cells, and Fresh and Fixed Tissue." *Nature Protocols* 7(5):872–81.

Zuellig, R. A., T. Hornemann, A. Othman, A. B. Hehl, H. Bode, T. Guntert, O. O. Ogunshola, E. Saponara, K. Grabliauskaite, J. H. Jang, U. Ungethuem, Y. Wei, A. von Eckardstein, R. Graf, and S. Sonda. 2014. "Deoxysphingolipids, Novel Biomarkers for Type 2 Diabetes, Are Cytotoxic for Insulin-Producing Cells." *Diabetes* 63(4):1326–39.